EC
Journals.ASM.org

Pleiotropic Roles of the Msi1-Like Protein Msl1 in *Cryptococcus neoformans*

Dong-Hoon Yang,[a] Shinae Maeng,[a] Anna K. Strain,[b] Anna Floyd,[c] Kirsten Nielsen,[b] Joseph Heitman,[c] and Yong-Sun Bahn[a]

Department of Biotechnology, Center for Fungal Pathogenesis, Yonsei University, Seoul, South Korea[a]; Department of Microbiology, Medical School, University of Minnesota, Minneapolis, Minnesota, USA[b]; and Departments of Molecular Genetics and Microbiology, Medicine, and Pharmacology and Cancer Biology, Duke University Medical Center, Durham, North Carolina, USA[c]

Msi1-like (MSIL) proteins contain WD40 motifs and have a pleiotropic cellular function as negative regulators of the Ras/cyclic AMP (cAMP) pathway and components of chromatin assembly factor 1 (CAF-1), yet they have not been studied in fungal pathogens. Here we identified and characterized an MSIL protein, Msl1, in *Cryptococcus neoformans*, which causes life-threatening meningoencephalitis in humans. Notably, Msl1 plays pleiotropic roles in *C. neoformans* in both cAMP-dependent and -independent manners largely independent of Ras. Msl1 negatively controls antioxidant melanin production and sexual differentiation, and this was repressed by the inhibition of the cAMP-signaling pathway. In contrast, Msl1 controls thermotolerance, diverse stress responses, and antifungal drug resistance in a Ras/cAMP-independent manner. Cac2, which is the second CAF-1 component, appears to play both redundant and distinct functions compared to the functions of Msl1. Msl1 is required for the full virulence of *C. neoformans*. Transcriptome analysis identified a group of Msl1-regulated genes, which include stress-related genes such as *HSP12* and *HSP78*. In conclusion, this study demonstrates pleiotropic roles of Msl1 in the human fungal pathogen *C. neoformans*, providing insight into a potential novel antifungal therapeutic target.

Msi1-like (MSIL) proteins belong to the family of WD40 motif-containing proteins discovered in a wide variety of eukaryotes ranging from yeasts to humans. WD40 repeat domains (also known as WD or β-transducin repeats) consist of approximately-40-amino-acid motifs with a terminal Trp-Asp (WD) dipeptide. WD40-containing proteins harbor 4 to 16 repeating units and are involved in eukaryotic signal transduction systems, and a paradigmatic example is the Gβ subunits of heterotrimeric G proteins (11). Most MSIL proteins have seven WD40 domains, which are thought to form a β-propeller structure through which a variety of protein-protein interactions can be mediated (39). In most MSIL-containing eukaryotes, two or more MSIL proteins are expressed, but some species have only one MSIL protein. The budding and fission yeast MSIL proteins, such as Msi1/Cac3 and Hat2 in *Saccharomyces cerevisiae* and Prw1 in *Schizosaccharomyces pombe*, are not essential. In contrast to eukaryotes, there are no known prokaryotic MSIL proteins, suggesting that MSIL proteins have eukaryote-specific cellular functions (16).

Regardless of the absence of any catalytic activity, MSIL proteins are known to play multiple roles in eukaryotes. The prototypical MSIL protein is Msi1 (multicopy suppressor of the *ira1* mutation 1) in *S. cerevisiae*. As reflected by its name, the multicopy expression of *MSI1* suppresses phenotypes resulting from the hyperactivation of the Ras/cyclic AMP (cAMP) pathway by an *ira1* mutation, such as heat shock sensitivity (38). Although the precise regulatory mechanism via which Msi1 functions in the Ras/cAMP-signaling pathway in budding yeast is not completely understood, several lines of evidence indicate that Msi1 operates either between the Cyr1 adenylyl cyclase and protein kinase A (PKA) or downstream of PKA. *MSI1* overexpression suppresses the heat shock sensitivity caused by the deletion of two phosphodiesterases, Pde1 and Pde2, or by an activated *TPK2* allele but not by the deletion of the Bcy1 regulatory subunit of PKA, suggesting that Msi1 downregulates Ras/cAMP signaling by inhibiting PKA in a Bcy1-dependent manner (21, 46). Supporting this, Msi1 does not inhibit intracellular cAMP synthesis (46). Interestingly, however, Msi1 also does not affect total PKA catalytic activity, indicating that Msi1 may affect the subcellular localization of PKA (46). In addition, Msi1 was found to negatively regulate the Ras/cAMP pathway by sequestering and inactivating the Npr1 serine/threonine kinase, which is known to promote or antagonize the ubiquitin-mediated degradation of several nutrient transporters (21). Indeed, *MSI1* overexpression phenotypes are strikingly similar to those of an *npr1*Δ mutant. On the other hand, *MSI1* overexpression also suppresses heat shock sensitivity caused by a loss of the Yak1 kinase, which is a downstream target of PKA but which antagonizes the Ras/cAMP pathway in an autoregulatory loop (34). Therefore, how Msi1 regulates the Ras/cAMP pathway in yeast remains elusive. Although Ras signaling is not mediated by cAMP in multicellular eukaryotes, an Msi1 homolog was also shown to antagonize Ras-mediated signaling in both *Caenorhabditis elegans* and humans (19, 30, 40). Furthermore, the overexpression of either RbAp48 or RbAp46, mammalian Msi1 homologs, suppresses the heat shock sensitivity of hyperactive Ras/cAMP yeast mutants (36, 37). Therefore, MSIL proteins are likely to negatively regulate Ras signaling in both unicellular and multicellular eukaryotes.

As a second cellular function, the MSIL proteins serve as a component of chromatin assembly factor 1 (CAF-1), which assembles histones H3 and H4 onto newly replicated DNA (24, 44). Therefore, yeast Msi1 is also known as Cac3 (chromatin assembly

Received 21 September 2012 **Accepted** 2 October 2012
Published ahead of print 5 October 2012
Address correspondence to Yong-Sun Bahn, ysbahn@yonsei.ac.kr.
Supplemental material for this article may be found at http://ec.asm.org/.
Copyright © 2012, American Society for Microbiology. All Rights Reserved.
doi:10.1128/EC.00261-12

complex 3). The CAF-1 complex is conserved from yeast to humans and consists of three proteins, Rlf2/Cac1, Cac2, and Msi1/Cac3, which correspond to p150, p60, and p48, respectively, in human CAF-1. To form the CAF-1 complex, Cac2 and Msi1/Cac3 bind to the larger component Rlf2/Cac1, but there is no direct interaction between Cac2 and Msi1/Cac3 (19). Both the regulation and localization patterns of Msi1/Cac3 are distinct from those of Rlf2/Cac1 and Cac2 (21, 41), in accordance with the multiple functional roles of Msi1/Cac3. In *S. cerevisiae*, the disruption of the genes encoding any of the three CAF-1 proteins causes multiple phenotypes, including increased UV sensitivity, a derepressed expression of genes located in heterochromatin and the silent mating-type loci, and a mislocalization of the telomere-binding protein Rap1 (13, 24). However, the function of CAF-1 is independent of the role of Msi1/Cac3 in negatively regulating the Ras/cAMP pathway in yeast (21, 46).

Besides these functions, MSIL proteins play additional roles. Msi1/RbAp48 serves as a corepressor for the retinoblastoma susceptibility gene product (pRB), which is a well-known tumor suppressor protein that represses the expression of S-phase genes during the G_1 phase of the cell cycle by inhibiting E2F transcription factors (25, 42). Interestingly, the corepressor activity of Msi1/Cac3 for pRB does not require Cac2, indicating that CAF-1 is not involved in this process. In *Arabidopsis*, the MSI1 protein interacts *in vivo* with the pRB homolog retinoblastoma-related 1 (Rbr1) and downregulates *MET1*, encoding DNA methyltransferase 1, which subsequently controls the genomic imprinting that determines parental allele-specific expression during early development (22).

MSIL proteins have not been studied in fungal pathogens thus far. Among MSIL-related signaling pathways, the Ras and cAMP signaling pathways have been well characterized in pathogenic fungi such as *Aspergillus fumigatus*, *Candida albicans*, and *Cryptococcus neoformans* (for reviews, see references 8 and 27). The Ras and cAMP pathways play critical roles in the cellular proliferation, differentiation, and virulence of pathogenic fungi. In *C. neoformans*, however, the Ras- and cAMP-signaling pathways are not closely related like those in *S. cerevisiae*. The major roles of the cAMP/PKA pathway are the regulation of two major virulence factors, the antiphagocytic capsule and antioxidant melanin, and sexual differentiation (2, 4, 6, 12, 17). The cAMP/PKA pathway plays a minor role in the defense against the heavy metal cadmium and the toxic metabolite methylglyoxal but plays a significant role in resistance to antifungal polyene drugs in *C. neoformans* (31). In contrast, the Ras-signaling pathway governs thermotolerance and invasive growth, which are critical for *C. neoformans* to survive inside the host, and morphological differentiation, including mating and monokaryotic fruiting/unisexual reproduction (1). Interestingly, Ras1 controls these phenotypes in a cAMP-dependent (invasive growth and mating), pheromone-responsive mitogen-activated protein kinase (MAPK)-dependent (mating), or Cdc24/Cdc42/Rac1-dependent (thermotolerance) manner (1, 33, 43, 45). The guanine nucleotide exchange factor (GEF) Cdc24 and the Rho-GTPase Cdc42 are Ras effector proteins that control growth at high temperatures and also play roles in the defense against osmotic, oxidative, genotoxic, and cell wall/membrane stress agents in *C. neoformans* in a cAMP-independent manner (31, 33). However, how the MSIL proteins are related to these signaling pathways in this fungal pathogen remains unknown.

In this study, we identified an Msi1-like protein, Msl1, in *C. neoformans* and functionally characterized it by connection to another potential CAF-1 component, Cac2, and Ras/cAMP-signaling pathways. By comparative phenotypic analyses of *msl1*Δ mutants and *ras1*Δ and cAMP-signaling mutants, we have found that Msl1 plays pleiotropic roles in regulating the production of the antioxidant melanin, sexual differentiation, and diverse stress responses, including thermotolerance, in a manner distinct from the Ras- and cAMP-signaling pathways. Msl1 appears to have both redundant and distinct functions with Cac2. Importantly, Msl1 is required for the full virulence of *C. neoformans*. Finally, we have identified a group of Msl1-regulated genes via DNA microarray-based transcriptome analyses. Therefore, this study provides a first comprehensive report of the roles of the MSIL protein and CAF-1 in a pathogenic fungus of global importance.

MATERIALS AND METHODS

Strains and growth media. *C. neoformans* strains used in this study are listed in Table S1 in the supplemental material. The strains were cultured on YPD (yeast extract-peptone-dextrose) medium unless indicated otherwise. Niger seed and L-3,4-dihydroxyphenylalanine (L-DOPA) media, used for melanin production; liquid L-DOPA medium, used for laccase assays; agar-based DME (Dulbecco's modified Eagle's) medium, used for capsule production; and V8 medium containing 5% V8 juice (Campbell's Soup Co.), used for mating, were made as previously described (2, 6, 15, 18).

Phylogenetic analysis. Protein sequences used for phylogenetic analysis were retrieved from the NCBI database and aligned by using CLUSTAL X v1.83. The phylogenetic tree was generated by implementing the Web-based Phylodendron Phylogenetic Tree Printer tool (http://iubio.bio.indiana.edu/treeapp/treeprint-form.html).

Construction of the *msl1*Δ mutant and its complemented strain. The *MSL1* gene (CNAG_03297.2) was disrupted in *C. neoformans* serotype A *MAT*α strain H99 and its congenic *MAT***a** strain KN99**a** with a disruption cassette generated via overlap PCR and by biolistic transformation, as previously described (5, 10). Primer sequences are provided in Table S2 in the supplemental material. Primers for the amplification of the 5′ and 3′ flanking regions of the *MSL1* gene were JOHE10425/JOHE10426 and JOHE10427/JOHE10428, respectively. M13 reverse and forward primers were used to amplify the Nat^r or Neo^r dominant selectable marker. Stable transformants were selected on YPD medium containing nourseothricin or G418. The *msl1*Δ mutant strain was confirmed both by diagnostic PCR using primer pair JOHE8994/JOHE10429 and by Southern blot analysis using a gene-specific probe prepared with PCR and primer pair JOHE11454/JOHE11455 (see Fig. S1B in the supplemental material). To verify *msl1*Δ mutant phenotypes, the *msl1*Δ+*MSL1* complemented strains were constructed as follows. First, H99 genomic DNA containing the full-length *MSL1* gene was isolated from a *C. neoformans* H99 bacterial artificial chromosome (BAC) library. By using the BAC clones as templates, a 3.1-kb fragment containing the complete *MSL1* gene, the 0.9-kb promoter region, and the 0.5-kb 3′-untranslated region (UTR) was amplified by PCR with primer pair B5/B6 and cloned into the pJET1/blunt vector (Fermentas Life Sciences), generating plasmid pJET1-MSL1. After confirming the DNA sequence, the insert was subcloned into pJAF12 (NEO^r), generating plasmid pNEOMSL1. For the targeted reintegration of the *MSL1* wild-type (WT) allele into its native locus, pNEOMSL1 was linearized by NdeI digestion, and *msl1*Δ strain YSB13 was biolistically transformed. The *cac1*Δ *msl1*Δ and *pka1*Δ *msl1*Δ mutant strains were produced by transforming the *cac1*Δ (YSB42) and *pka1*Δ (YSB188) mutants with the *msl1*Δ::*NEO* allele. The mutants were confirmed by diagnostic PCR and Southern blotting using the same primer sets and probe utilized for the *msl1*Δ mutant (see Fig. S2C in the supplemental material).

Construction of the *cac2*Δ mutant. The *CAC2* gene (CNAG_00718.2) was disrupted as follows. Primer pairs used for the amplification of the 5′ and 3′ flanking regions of the *CAC2* gene were B1927/B1928 and B1929/B1930, respectively. The NEO^r dominant marker was used for the *CAC2* disruption.

To identify the desired *cac2*Δ mutant, diagnostic PCR with primer pair JOHE8994/B1931 and Southern blot analysis with a gene-specific probe PCR amplified with primer pair B1927/B1932 were performed (see Fig. S3B in the supplemental material).

Localization study of Msl1. The *msl1*Δ+*MSL1-GFP* strain was constructed as follows. The promoter and the entire open reading frame (ORF) region of *MSL1* were amplified by PCR with H99 genomic DNA as the template and primers B4112 and B4113 containing the linker sequence 5′-GGTGGCGGTGGCTCT-3′ and cloned into plasmid pTOP-V2 (Enzynomics). After sequence confirmation, this fragment was released with XhoI and XmaI and subcloned into pJAF12 (NEO^r) to produce pJAF12-MSL1. The green fluorescent protein (GFP) gene was amplified by PCR with plasmid pACT-HOG1fGFP as the template and primers B4114, containing an XmaI site, and B4115. The *MSL1* terminator region was amplified by PCR with primers B4116 and B4545, containing a NotI site. The *GFP-MSL1* terminator cassette was amplified by overlap PCR with primers B4114 and B4545, digested with XmaI and NotI, and subcloned into an XmaI/NotI-digested pJAF12-MSL1 plasmid, generating pJAF12-MSL1::GFP. After sequence confirmation of the *GFP* gene and *MSL1* terminator region, the pJAF12-MSL1::GFP plasmid was linearized with XbaI, and *msl1*Δ mutant strain YSB13 was biolistically transformed. The targeted reintegration of the *MSL1*::*GFP* allele into the native *MSL1* locus was confirmed by diagnostic PCR (data not shown). To observe Msl1 protein localization, the *msl1*Δ+*MSL1*::*GFP* strain was incubated overnight at 30°C in 50 ml YPD medium, and 5 ml of culture was inoculated into 45 ml of fresh YPD medium and incubated until the optical density at 600 nm (OD_{600}) reached approximately 1.0. One milliliter of culture was sampled at time zero, and the remaining culture was shifted to a higher temperature (37°C), or 7 μg/ml of thiabendazole (TBZ) or 2.5 mM diamide was added. One milliliter of the culture was sampled after 30 or 60 min of incubation and fixed according to a method recommended by the Koshland laboratory (http://mcb.berkeley.edu/labs/koshland/Protocols/MICROSCOPY/gfpfix.html). First, cells were spun down, and the supernatant was removed. One hundred microliters of 4% paraformaldehyde containing 3.4% sucrose was added to the sample, and the sample was incubated for 15 min at room temperature. After incubation, cells were spun down and washed with 500 μl of 0.1 M potassium phosphate buffer adjusted to pH 7.5 and containing 1.2 M sorbitol. Fixed cells were permeabilized by resuspending them in an equal volume of phosphate-buffered saline (PBS) containing 1% Triton X-100 for 5 min. After permeabilization, cells were washed and resuspended in PBS. Five microliters of sample was mixed with 5 μl of 2 μg/ml 4′,6-diamidino-2-phenylindole (DAPI) and incubated for 1 h. After incubation, samples were mixed with 10 μl of mounting medium (Biomeda) and then visualized with a Nikon eclipse Ti microscope.

Construction of a constitutive *MSL1* overexpression strain. A constitutive *MSL1* overexpression strain was constructed by using the histone H3 promoter of *C. neoformans* serotype D strain JEC21. The left flanking region (the *MSL1* promoter region spanning positions −1029 to −1 relative to the ATG start codon [positions +1 to +3]) and the right ORF region (*MSL1* gene, positions +1 to + 915) were PCR amplified with primer pairs B4019/B4020 and B4021/B4022, respectively. The *NAT*-H3 promoter or *NEO*-H3 promoter fragment was PCR amplified with primer pair B4017/B4018. The P_{H3}::*MSL1* allele cassette was generated by overlap PCR with two primers, B4019 and B4022, and gel extracted, and *C. neoformans* serotype A *MAT*α strain H99, the *cac1*Δ strain (YSB42), or the *pka1*Δ strain (YSB188) was biolistically transformed. Stable transformants were selected on YPD medium containing nourseothricin or G418. The P_{H3}::*MSL1* strains were screened by diagnostic PCR and Southern blot analysis using an *MSL1*-specific probe generated by PCR with primers JOHE11454 and JOHE11455. The expression levels of *MSL1* in P_{H3}::*MSL1* strains were measured by Northern blot analysis using an *MSL1*-specific probe amplified by PCR with primers B3513 and B3514.

Assays for capsule and melanin production and mating. The qualitative visualization and quantitative measurement of capsule and melanin production were performed as described previously (6, 18, 23). Mating assays were also performed as described previously (6, 18). Images of mating were captured with a Nikon Eclipse E400 microscope equipped with a Nikon DXM1200F digital camera.

Stress and antifungal drug sensitivity test. Each strain was incubated overnight at 30°C in YPD medium, serially diluted (1 to 10^4 dilutions) in distilled water (dH_2O), and spotted (3 μl) onto solid YPD medium. The cells were then spotted onto YPD medium containing the indicated concentration of diamide, *tert*-butyl hydroperoxide (tBOOH), or H_2O_2 for oxidative stress; amphotericin B (AMB), fluconazole (FCZ), itraconazole (ICZ), or ketoconazole (KCZ) for antifungal drug tests; methyl methane sulfonate (MMS), hydroxyurea (HU), or TBZ for genotoxic stress; or cadmium sulfate ($CdSO_4$) for toxic heavy metal stress. For UV sensitivity, cells spotted onto solid YPD medium were exposed to UV at 250 J/m^2, 350 J/m^2, or 450 J/m^2 by using a UV Stratalinker instrument (model 2400; Stratagene). To test temperature sensitivity, plates were incubated at 30°C, 37°C, or 39°C. To test osmosensitivity, cells grown overnight in YPD medium were spotted onto solid yeast extract-peptone (YP) and YPD medium containing 1 M or 1.5 M NaCl or KCl. Each plate was incubated for 2 to 7 days and photographed.

Transcriptome analysis by DNA microarray. Total RNA of the wild type and the *msl1*Δ mutant strain (YSB13) was isolated as follows. Cells were cultured in 50 ml YPD medium at 30°C for 16 h. Five milliliters of this culture was diluted 1/20 with 95 ml fresh YPD medium and further cultured at 30°C until the OD_{600} reached approximately 1.0. The cultures were then immediately frozen in liquid nitrogen and lyophilized overnight. Three independent cultures for each strain were prepared for total RNA preparation as biological replicates for DNA microarray analysis. Total RNA was prepared by using TRIzol reagent, as previously described (26). For control total RNA, all of the total RNAs prepared from WT and mutant cells were pooled (pooled reference RNAs). For cDNA synthesis, Cy5/Cy3 labeling, prehybridization, hybridization, and slide washing, we followed protocols described previously (26). For DNA microarray slides, we utilized *C. neoformans* serotype D 70-mer oligonucleotide microarray slides containing 7,936 spots (Duke University) by mapping the serotype A gene ID database to each corresponding 70-mer oligonucleotide sequence of the array (26). Three independent DNA microarrays with three independent biological replicates were performed. The DNA microarray slides were scanned with a GenePix 4000B scanner (Axon Instrument), and the scanned images were analyzed with GenePix Pro (version 4.0) and a gal file (http://genome.wustl.edu/activity/ma/cneoformans). For hierarchical and statistical analysis, data transported from GenePix software were analyzed with Acuity software by employing locally weighted scatterplot smoothing (LOWESS) normalization, reliable gene filtering (>95% filtering), hierarchical clustering, zero transformation, and analysis of variance (ANOVA) ($P < 0.05$) and with Microsoft Excel software.

Northern blot analysis and quantitative real-time reverse transcription-PCR. Quantitative real-time reverse transcription-PCR (qRT-PCR) for the quantitative measurement of the relative expression levels of Msl1-regulated genes, including *HSP78*, *SNF3*, *SSL1*, and *HSP12*, was performed with primers listed in Table S2 in the supplemental material by using the SuperScript II reverse transcriptase system, as described previously (26). *ACT1* was used for the normalization of gene expression levels. Northern blot analysis to monitor the expression levels and patterns of *MSL1*, *HSP12*, and *HSP78* was performed as described previously (23).

Animal studies. The wild-type strain (H99), the *msl1*Δ mutant (YSB13), and the *msl1*Δ+*MSL1* complemented strain (YSB528) were cultured overnight in YPD broth. The resulting yeast cells were pelleted and resuspended in sterile PBS at a concentration of 1×10^6 cells/ml based on hemocytometer counting. Groups of 10 7-week-old female A/J mice (Jackson Laboratories, Bar Harbor, ME) were anesthetized by intraperitoneal pentobarbital injection. Animals were infected intranasally with 5×10^4 cells in 50 μl PBS. The concentration of cells in the inoculum was confirmed by plating serial dilutions and enumerating CFU. Mice were monitored daily, and those that showed signs of severe morbidity (weight

loss, extension of the cerebral portion of the cranium, abnormal gait, paralysis, seizures, convulsion, or coma) were sacrificed by CO_2 inhalation. Organs from 3 to 5 mice per strain were also analyzed for CFU at the time of sacrifice. The lungs, spleen, and brain were harvested and homogenized in 2 to 4 ml PBS, and serial dilutions were plated onto YPD medium. The Mann-Whitney U test was performed to analyze differences between survival curves, and P values of <0.05 were considered significant.

Microarray data accession number. The entire microarray data set generated in this study was submitted to the Gene Expression Omnibus (GEO) (http://www.ncbi.nlm.nih.gov/geo/) under accession number GSE40303.

RESULTS

Identification of an Msi1-like protein in *C. neoformans*. To search for an MSIL ortholog in *C. neoformans*, a BLAST search (tblastn) of the *C. neoformans* var. *grubii* (serotype A strain H99) genome database was performed, using the Msi1/Cac3 protein sequence of *S. cerevisiae*. Based on the database, the serotype A *C. neoformans* genome contains a gene (CNAG_03297.2) that is predicted to encode a 435-amino-acid protein, which shares 29% identity and 47% similarity with the *S. cerevisiae* Msi1/Cac3 protein (tblastn score of 188.734 and expectancy value of 0.0). To confirm this, we performed 5′- and 3′-rapid amplification of cDNA ends (RACE) and whole-cDNA analysis. The RACE analysis revealed that CNAG_03297.2 contains 108-bp and 116-bp 5′- and 3′-untranslated regions (UTRs), respectively, and a 1,305-bp coding sequence spanning 10 exons, which encodes a 435-amino-acid protein product (GenBank accession no. JQ004401). The ORF size and genomic DNA structure are equivalent to those predicted by the H99 genome database. *C. neoformans* var. *neoformans* (serotype D strain JEC21) also contains a single copy of the Msi1 ortholog that is 98% identical to the serotype A Msi1 ortholog in predicted amino acid sequence. Notably, the *C. neoformans* Msi1 ortholog is more homologous to the mammalian retinoblastoma-binding proteins RbAp48 (51% identity) and RbAp46 (50% identity) than to the *S. cerevisiae* Msi1 ortholog (Fig. 1A). The phylogenetic analysis revealed that most of the MSIL proteins found in basidiomycetes are generally more homologous to their human orthologs than to those found in other fungal phyla (Fig. 1A).

Compared to RbAp46/RbAp48, which has seven WD40 domains, the *C. neoformans* Msi1 ortholog contains six WD40 domains that correspond to the second to seventh WD domains of the human MSIL proteins in domain position (Fig. 1B; see also Fig. S1 in the supplemental material). Although it harbors the first WD40-like domain, a terminal WD or FD dipeptide was not conserved. Similarly, *S. cerevisiae* Msi1 also contains six WD40 domains with one less-conserved fourth WD40 domain, whereas *S. pombe* Prw1 and Mis16 have five WD40 domains with two less-conserved WD40 domains at the first and fourth positions (Fig. 1B). Notably, the terminal WD or FD dipeptides are even less conserved in *C. albicans* (Fig. 1B; see also Fig. S1 in the supplemental material). In summary, *C. neoformans* contains a single Msi1 ortholog with six WD40 domains and a single WD40-like domain. Therefore, we named this *C. neoformans* gene *MSL1* (*MSI1*-like gene 1).

Temperature-dependent growth requirement for Msl1. To elucidate the potential role of Msl1 in *C. neoformans*, we constructed *msl1*Δ mutants of serotype A strains H99 (*MAT*α) and KN99**a** (*MAT***a**) and performed comparative phenotypic analyses of these mutants with Ras- and cAMP/PKA-signaling mutants that we previously isolated and characterized in the same H99 and KN99**a** genetic background (6, 7). We deleted 1,559 bp of the 1,784-bp genomic ORF DNA of *MSL1* (positions +180 to +1737) with the *msl1*Δ::*NAT* or *msl1*Δ::*NEO* allele (see Fig. S2A and S2B in the supplemental material). To verify the phenotypes of the *msl1*Δ mutant, an *msl1*Δ+*MSL1* complemented strain was constructed by reintegrating the WT *MSL1* gene into its native locus. Furthermore, in order to address the genetic and functional relationships between Msl1 and the Ras/cAMP-signaling pathways, we deleted the *MSL1* gene in *C. neoformans* cells having a mutation in the *RAS1* gene, the adenylyl cyclase gene (*CAC1*), or a major catalytic subunit of protein kinase A (*PKA1*), generating the *msl1*Δ *ras1*Δ, *msl1*Δ *cac1*Δ, and *msl1*Δ *pka1*Δ double mutants, respectively (see Fig. S2C in the supplemental material).

The deletion of *MSL1* did not affect the normal growth of *C. neoformans* under nutrient-rich, unstressed growth conditions at 30°C (Fig. 2A). At elevated temperatures, however, the *msl1*Δ mutant exhibited discernible growth defects. The *msl1*Δ mutant showed a minor growth defect at 37°C, and this temperature-sensitive (TS) growth defect was even more pronounced at 39°C (Fig. 2A). Confirming that this phenotype is attributable to the *msl1*Δ mutation, the TS growth defect of the *msl1*Δ mutant was restored by the reintegration of the WT *MSL1* gene. The deletion of either *CAC1* or *PKA1* did not affect the TS phenotype of the *msl1*Δ mutant (Fig. 2A), indicating that Msl1 exhibits a cAMP/PKA-independent phenotype in thermotolerance. The *msl1*Δ mutant exhibited less-severe TS growth defects than the *ras1*Δ mutant. Notably, the *msl1*Δ *ras1*Δ mutant showed significant growth defects even at 30°C and severe thermosensitivity at 37°C or 39°C (Fig. 2A).

Increased thermosensitivity is often linked to weakened cell membrane stability. Therefore, many TS mutants also exhibit hypersensitivity to membrane-destabilizing agents such as SDS. In fact, the deletion of *MSL1* significantly increased SDS sensitivity in both WT and cAMP mutant (*cac1*Δ and *pka1*Δ) backgrounds (Fig. 2B). In response to SDS, the *msl1*Δ *ras1*Δ mutant appeared to show even greater sensitivity than each single mutant (Fig. 2B). These data suggest that Msl1- and Ras-signaling pathways independently control the growth, thermotolerance, and cell membrane stability of *C. neoformans*.

Msl1 regulates production of antioxidant melanin but not antiphagocytic capsule. To further address whether Msl1 is involved in the regulation of the Ras- or cAMP-signaling pathways, we analyzed various phenotypes known to be controlled by the two signaling pathways. These phenotypes include the production of the antioxidant melanin and the polysaccharide capsule, sexual differentiation, the stress response, and the virulence of *C. neoformans*.

First, we monitored melanin biosynthesis, which is positively regulated by the cAMP-signaling pathway. Under glucose-starved conditions, the cAMP-signaling pathway is activated to induce laccase genes, such as *LAC1*, which catalyze the biosynthesis of the antioxidant pigment melanin (9, 20, 28, 32). Because the TS growth defect of the *msl1*Δ mutant may affect melanin synthesis levels at the usual assay temperature of 37°C, we monitored melanin synthesis at 30°C. As previously reported (6), the *aca1*Δ and *gpa1*Δ mutants were partially defective in melanin production, whereas the *cac1*Δ mutant was severely deficient in melanin production in L-DOPA-containing medium (Fig. 3A). The *ras1*Δ mutant was also slightly defective in melanin production (Fig. 3A).

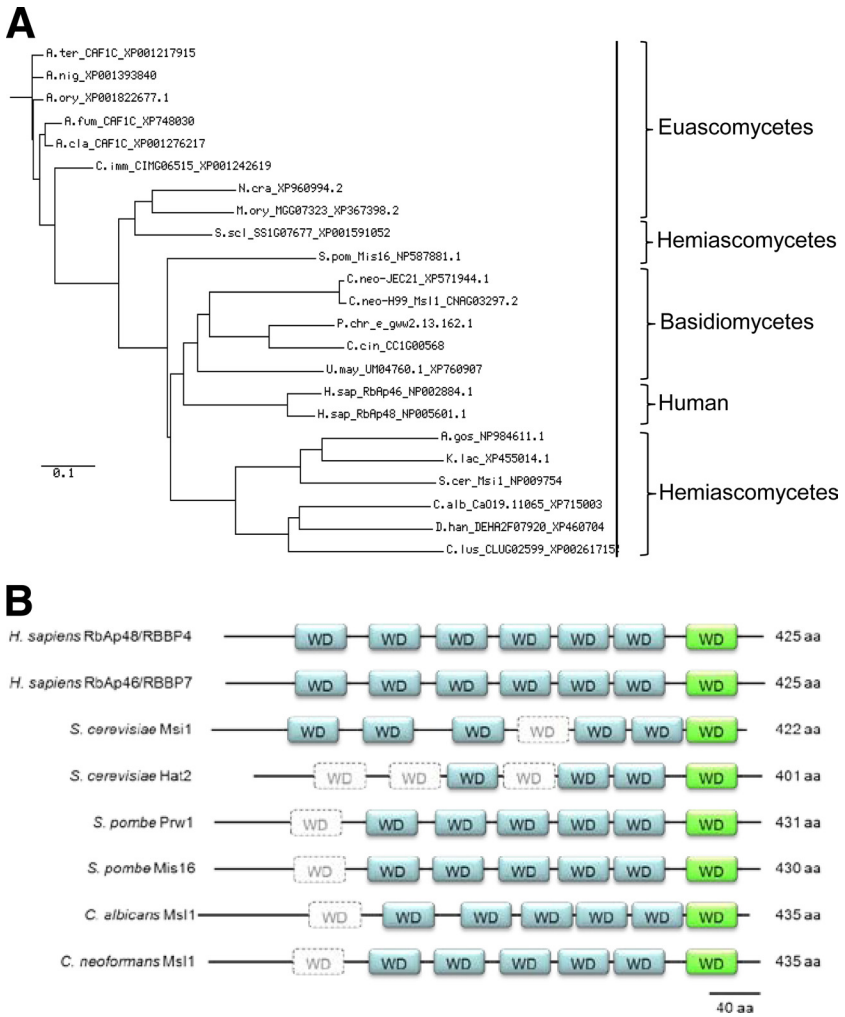

FIG 1 Identification of the *C. neoformans MSL1* gene. (A) Phylogenetic analysis of MSIL proteins in fungi and humans. The phylogenetic tree was drawn with the Phylodendron Phylogenetic Tree Printer (http://iubio.bio.indiana.edu/treeapp/treeprint-form.html). The scale bar depicts an evolutionary distance of 0.1. A.ter, *Aspergillus terreus*; A.nig, *Aspergillus niger*; A.ory, *Aspergillus oryzae*; A.cla, *Aspergillus clavatus*; C.imm, *Coccidioides immitis*; N.cra, *Neurospora crassa*; M.ory, *Magnaporthe oryzae*; S.scl, *Sclerotinia sclerotiorum*; P.chr, *Phanerochaete chrysogenum*; C.cin, *Coprinopsis cinerea*; U.may, *Ustilago maydis*; A.gos, *Ashbya gossypii*; K.lac, *Kluyveromyces lactis*; D.han, *Debaryomyces hansenii*; C.lus, *Candida lusitaniae*. (B) Conserved WD40 domains in MSIL proteins. The WD40 domains of each protein were identified by alignment and sequence comparison of MSIL proteins. The blue box indicates conserved WD40 domains with a terminal WD dipeptide. The box with dashed lines indicates WD40-like domains that do not contain the terminal WD dipeptide. The green box indicates the last WD40 domains that contain a WX (Trp random amino acid) terminal sequence. aa, amino acids.

During incubation on melanin-inducing medium (L-DOPA), the *msl1*Δ mutant showed slightly increased melanin production compared to that of the WT (Fig. 3A). The complementation of the *msl1*Δ mutant with *MSL1* restored melanin production to WT levels (Fig. 3A). A quantitative measurement of melanin production also confirmed this finding (Fig. 3B). The increased melanin production in the *msl1*Δ mutant may result from an enhanced induction of *LAC1*, encoding laccase, whose expression is induced under carbon-starved conditions (no glucose) in *C. neoformans*. Indeed, *LAC1* was induced more robustly in the *msl1*Δ mutant than in the wild type (Fig. 3C). The disruption of *CAC1* or *PKA1*, encoding an adenylyl cyclase and protein kinase A (PKA), respectively, abolished melanin production in the *msl1*Δ mutant (Fig. 3D). These data indicate that Msl1 may negatively control melanin production upstream of Cac1 and Pka1 in the cAMP-signaling pathway.

Next, we addressed the role of Msl1 in capsule production, which is also positively regulated by the cAMP-signaling pathway (3, 6, 35). Here we also measured relative capsule production levels in the *msl1*Δ mutant at 30°C to eliminate any possibility of an involvement of its TS phenotype in capsule synthesis. The *msl1*Δ mutant showed WT levels of capsule by both quantitative and qualitative measurements (Fig. 3E). Furthermore, the reduced capsule production observed for the *cac1*Δ and *pka1*Δ mutants was not altered by the deletion of *MSL1* (*cac1*Δ *msl1*Δ and *pka1*Δ *msl1*Δ double mutants). Due to its growth defect, a proper measurement of melanin and capsule biosynthesis was not possible for the *ras1*Δ *msl1*Δ mutant (data not shown). In summary, Msl1 controls melanin, but not capsule, negatively in a pattern distinct from the Ras- and cAMP-signaling pathways.

Msl1 is required for sexual differentiation of *C. neoformans*. Sexual differentiation resulting from mating between α and **a** strains is an important process for *C. neoformans* to generate in-

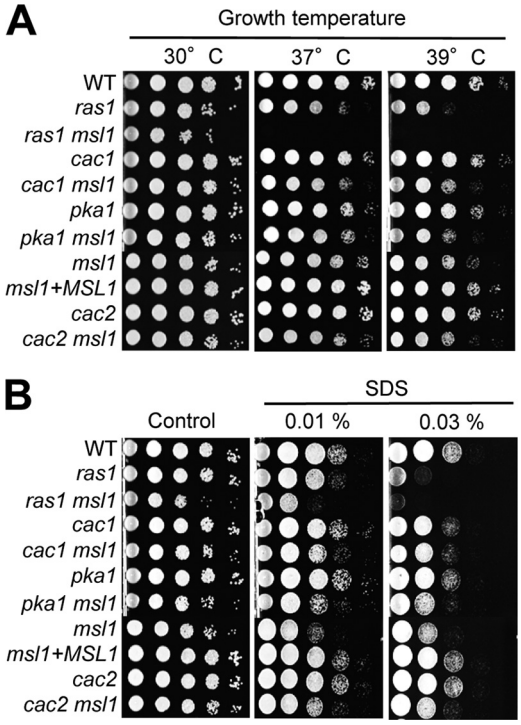

FIG 2 Msl1 is involved in thermotolerance and cell membrane stability. Each *C. neoformans* strain (WT strain H99 and *ras1*Δ [YSB53], *ras1*Δ *msl1*Δ [YSB1790], *cac1*Δ [YSB42], *cac1*Δ *msl1*Δ [YSB1084], *pka1*Δ [YSB188], *pka1*Δ *msl1*Δ [YSB1086], *msl1*Δ [YSB13], *msl1*Δ+*MSL1* [YSB528], *cac2*Δ [YSB1065], and *cac2*Δ *msl1*Δ [YSB1697] mutants) was grown overnight at 30°C in liquid YPD medium and 10-fold serially diluted (1 to 10^4 dilutions). (A) Diluted cells were spotted (3 μl of the dilution) onto YPD plates and further incubated at 37°C or 39°C for 2 days to monitor thermotolerance. (B) For measurements of cell membrane stability, cells were spotted onto YPD plates containing the indicated concentrations of SDS, further incubated at 30°C for 3 days, and photographed.

fectious propagules for host infection. This process is also positively regulated by the Ras- and cAMP-signaling pathways. In a unilateral cross between α *msl1*Δ and WT **a** (KN99**a**) strains, normal mating and filamentation were observed. In a bilateral cross between α *msl1*Δ and **a** *msl1*Δ mutant strains, however, mating appeared to be significantly enhanced (Fig. 4A). The reintegration of the WT *MSL1* gene into the α *msl1*Δ strain restored normal levels of mating with the **a** *msl1*Δ strain, further confirming that Msl1 negatively regulates the mating of *C. neoformans*.

To address whether the role of Msl1 in mating is mediated by the cAMP-signaling pathway, we crossed the α *pka1*Δ *msl1*Δ or α *cac1*Δ *msl1*Δ mutants with the **a** *msl1*Δ mutants. The deletion of either *CAC1* or *PKA1* completely abolished the mating capability of the *msl1*Δ mutant (Fig. 4B). Similarly, we also crossed the **a** *msl1*Δ mutants with the α *ras1*Δ *msl1*Δ mutant. Similar to the *CAC1* or *PKA1* deletion, the *RAS1* deletion also completely abolished the mating capability of the *msl1*Δ mutant (data not shown), although this mating defect may result from the growth defect of the α *ras1*Δ *msl1*Δ mutant. These results suggest that Msl1 negatively regulates the mating process of *C. neoformans*, possibly via the regulation of the Ras- and cAMP-signaling pathways.

Msl1 plays pleiotropic roles in the stress response of *C. neoformans*. The Ras- and cAMP-signaling pathways are involved in the stress response and antifungal drug susceptibility of *C. neoformans* (31). Therefore, we monitored various stress-related phenotypes and the antifungal drug resistance of the *msl1*Δ mutant compared with those of the Ras and cAMP signaling mutants. Besides thermosensitivity, the *ras1*Δ mutant is also hypersensitive to genotoxic stresses and DNA-damaging agents (31). Similar to the *ras1*Δ mutant, but distinct from the *cac1*Δ and *pka1*Δ mutants, the *msl1*Δ mutant exhibited increased sensitivity to diverse DNA-damaging agents, such as UV irradiation, hydroxyurea (HU), methyl methane sulfonate (MMS), and thiabendazole (TBZ) (Fig. 5A). The disruption of *MSL1* also increased the genotoxic stress sensitivity of the *cac1*Δ or *pka1*Δ mutant (Fig. 5A). Furthermore, the *ras1*Δ *msl1*Δ double mutant appeared to exhibit greater genotoxic sensitivity than each single mutant (Fig. 5A). In summary, Msl1 is involved in the genotoxic stress response in a Ras- and cAMP-independent manner, and the role of Msl1 in DNA damage repair appears to be conserved in *C. neoformans*.

In contrast to thermotolerance and genotoxic stress responses, Msl1 appeared to operate differently from Ras1 in oxidative and heavy metal stress responses. For an oxidative stress response test, we monitored cellular susceptibility to hydrogen peroxide (H_2O_2) and organic peroxide (*tert*-butyl hydroperoxide [tBOOH]), which oxidizes thiol groups of proteins and generates reactive radicals, and diamide, which is an exogenous oxidant that reacts with thiol groups of proteins and glutathiones. As reported previously (31), the *ras1*Δ mutant exhibited increased susceptibility to diamide (Fig. 5A). Conversely, the *msl1*Δ mutant displayed slightly greater resistance to diamide than the WT, similar to the *cac1*Δ and *pka1*Δ mutants (Fig. 5A). Notably, the deletion of *MSL1* further increased the diamide resistance of the *ras1*Δ, *cac1*Δ, and *pka1*Δ mutants (Fig. 5A), indicating that the role of Msl1 in diamide resistance is largely independent of the Ras- and cAMP-signaling pathways. In contrast to diamide, the deletion of *MSL1* slightly increased susceptibility to H_2O_2 and tBOOH in both WT and Ras/cAMP mutant backgrounds (Fig. 5A).

In the heavy metal stress response, the *msl1*Δ mutant also exhibited different phenotypes from those of the *ras1*Δ mutant. The *msl1*Δ mutant was slightly more resistant to cadmium sulfate ($CdSO_4$) than the WT, whereas the *ras1*Δ mutant was more susceptible (Fig. 5B). The deletion of *MSL1* also increased $CdSO_4$ resistance in the *ras1*Δ, *cac1*Δ, and *pka1*Δ mutants, further supporting the Ras/cAMP-independent role of Msl1 in the heavy metal stress response of *C. neoformans*. Taken together, Msl1 plays pleiotropic roles in diverse stress responses but in a manner independent of the Ras- and cAMP-signaling pathways.

Disruption of Msl1 promotes antifungal drug resistance. Previously, we showed that the HOG pathway represses ergosterol biosynthesis and, therefore, that its inhibition promotes polyene drug sensitivity but increases azole drug resistance (26). On the other hand, the Ras and cAMP pathways promote sensitivity to polyene drugs, but not to azole drugs, in a manner independent of ergosterol biosynthesis (31). Here we found that the deletion of *MSL1* slightly increased the resistance to azole drugs such as fluconazole (FCZ) and ketoconazole (KCZ) (Fig. 5C). Interestingly, this effect was more evident in the *cac1*Δ and *pka1*Δ mutant backgrounds. The *msl1*Δ *cac1*Δ and *msl1*Δ *pka1*Δ double deletion mutants exhibited a striking resistance to FCZ and KCZ (Fig. 5C). Regardless of the remarkably increased azole resistance, the *msl1*Δ *cac1*Δ and *msl1*Δ *pka1*Δ mutants did not show any increased amphotericin B (AMB) sensitivity (Fig. 5C). Indeed, the deletion of *MSL1* partly recovered AMB resistance in the *cac1*Δ and *pka1*Δ

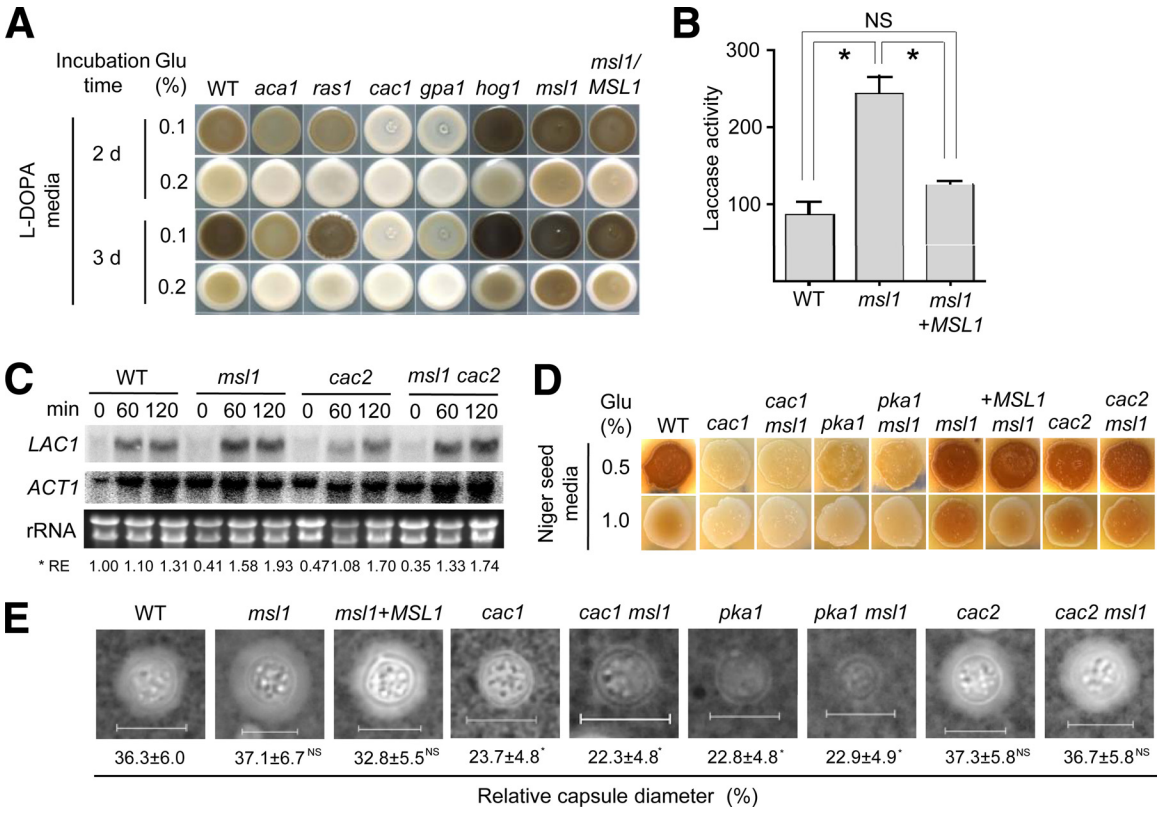

FIG 3 *MSL1* is required for melanin production but dispensable for capsule production. (A) The following strains were spotted and grown on L-DOPA agar medium (0.1% and 0.2% glucose) at 30°C for 3 days and photographed after 2 and 3 days: WT strain H99 and the *aca1*Δ (YSB6), *ras1*Δ (YSB53), *cac1*Δ (YSB42), *gpa1*Δ (YSB83), *hog1*Δ (YSB64), *msl1*Δ (YSB13), and *msl1*Δ+*MSL1* (YSB528) mutants. (B) Melanin production was quantitatively measured by a laccase assay. WT strain H99 and the *msl1*Δ (YSB13) and *msl1*Δ+*MSL1* (YSB528) mutants were cultured in liquid YPD medium overnight, diluted 1/20 with fresh YPD liquid medium, and further cultured until the OD_{600} reached about 1.0. These cells were transferred into liquid L-DOPA medium and cultured for 24 h in the dark. The OD_{475} of the culture supernatant was then measured. Laccase activity is described as units of laccase, in which 1 unit is defined as an OD_{475} of 0.001. (C) WT strain H99 and the *msl1*Δ (YSB13), *cac2*Δ (YSB1065), and *cac2*Δ *msl1*Δ (YSB1697) mutants grown to the logarithmic phase (OD_{600} = 1.0) in YPD liquid medium (time zero control) were shifted to yeast nitrogen base liquid medium lacking glucose and further incubated at 30°C. At the indicated time points, a portion of the cells was sampled, and their total RNA was isolated for Northern blot analysis. The membrane was hybridized with a *LAC1*-specific probe, washed, and developed with a phosphorimager. For the normalization of *LAC1* expression levels, the same membrane was stripped, rehybridized with the *ACT1*-specific probe, washed, and developed. The relative *LAC1* expression level (RE) at each time point indicates the normalized *LAC1* expression level compared to that at the zero time point for the wild-type sample. (D) The following strains were spotted and grown on Niger seed agar medium (0.5% and 1.0% glucose) at 30°C for 3 days and photographed: WT strain H99 and the *cac1*Δ (YSB42), *cac1*Δ *msl1*Δ (YSB1084), *pka1*Δ (YSB188), *pka1*Δ *msl1*Δ (YSB1086), *msl1*Δ (YSB13), *msl1*Δ+*MSL1* (YSB528), *cac2*Δ (YSB1065), and *cac2*Δ *msl1*Δ (YSB1697) mutants. (E) For capsule production, WT strain H99 and the *cac1*Δ (YSB42), *cac1*Δ *msl1*Δ (YSB1084), *pka1*Δ (YSB188), *pka1*Δ *msl1*Δ (YSB1086), *msl1*Δ (YSB13), *msl1*Δ+*MSL1* (YSB528), *cac2*Δ (YSB1065), and *cac2*Δ *msl1*Δ (YSB1697) mutants were spotted onto a DME agar plate and incubated at 30°C for 2 days. Scraped cells were resuspended in distilled water and visualized by India ink staining. The scale bars indicate 10 μm. The relative capsule diameter of each strain was measured by use of the following equation: (diameter of capsule − diameter of cell) × 100/diameter of capsule. Statistical differences among strains were determined by Bonferroni's multiple-comparison test. Asterisks and NS indicate a *P* value of <0.001 and a nonsignificant value, respectively.

mutants, although the *msl1*Δ mutant showed almost WT susceptibility to AMB (Fig. 5C). These data indicate that Msl1 controls azole and polyene drug resistance without an involvement of ergosterol biosynthesis and in a manner independent of the Ras- and cAMP-signaling pathways.

Expression patterns of *MSL1* and effects of *MSL1* overexpression in *C. neoformans*. Based on the pleiotropic roles of Msl1 in diverse stress responses and adaptation, we monitored whether *MSL1* is differentially regulated under different environmental conditions. In response to genotoxic agents (HU, MMS, or TBZ), the *MSL1* expression level was not significantly affected and indeed appeared to be slightly decreased (Fig. 6). In response to oxidative agents such as diamide, H_2O_2, or tBOOH, the *MSL1* expression level also appeared to be decreased. The reduction of the *MSL1* expression level was most evident in response to H_2O_2 (Fig. 6). In response to osmotic stresses (NaCl, KCl, or sorbitol), the *MSL1* expression level was either not affected significantly or slightly reduced (Fig. 6). Considering these expression patterns, the role of Msl1 in the stress response and adaptation is not likely to result from the differential expression of *MSL1*.

Next, we addressed whether the artificial overexpression of *MSL1* may oppositely affect phenotypes of the *msl1*Δ mutant. For this purpose, we constructed the P_{H3}::*MSL1* allele, where the histone 3 (H3) promoter, which is a constitutively expressed strong promoter in *C. neoformans*, was inserted upstream of the start codon of *MSL1* (see Fig. S4A in the supplemental material). We introduced the P_{H3}::*MSL1* allele into the wild-type strain and cAMP mutants (*cac1*Δ or *pka1*Δ mutants) (see Fig. S4B in the

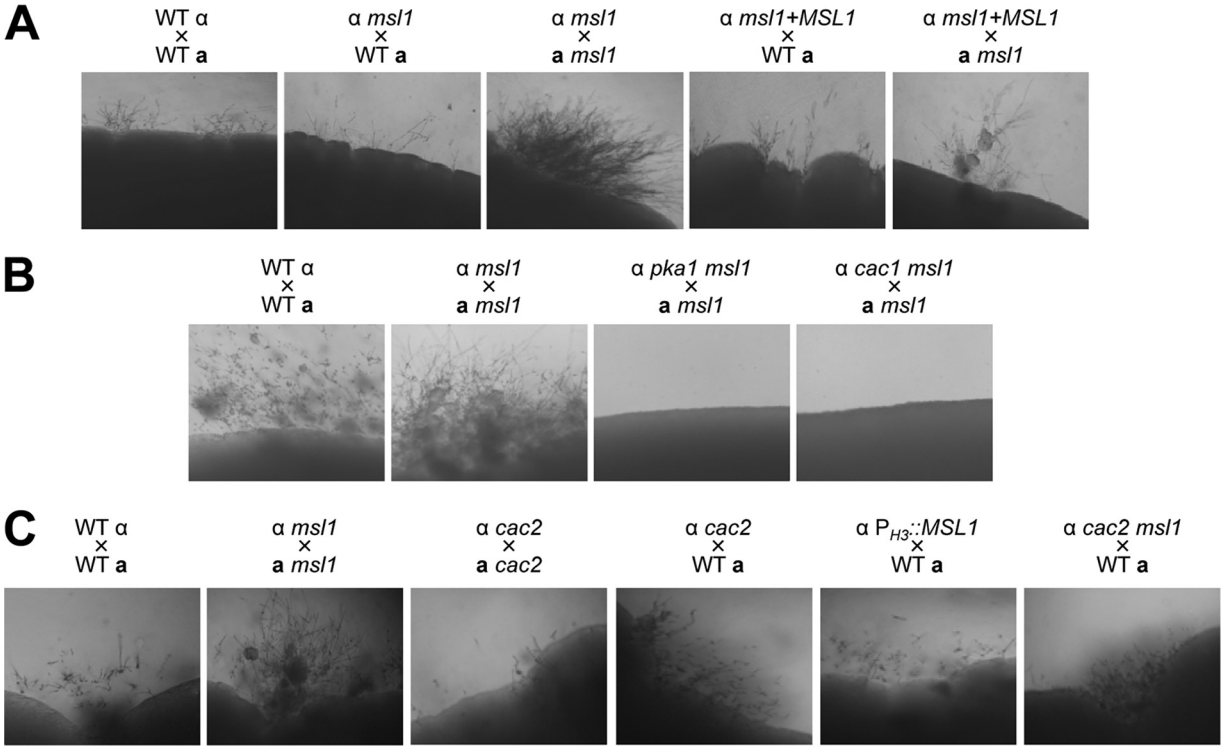

FIG 4 Msl1 negatively regulates sexual differentiation of *C. neoformans*. The following serotype A *C. neoformans* α and **a** strains were cocultured on V8 medium for 2 weeks at room temperature in the dark: WT α × WT **a** (H99 and KN99**a**), α *msl1* × WT **a** (YSB13 and KN99**a**), α *msl1* × **a** *msl1* (YSB13 and YSB62), α *msl1*+*MSL1* × WT **a** (YSB528 and KN99**a**), and α *msl1*+*MSL1* × **a** *msl1* (YSB528 and YSB62) (A); WT α × WT **a** (H99 and KN99**a**), α *msl1* × **a** *msl1* (YSB13 and YSB62), α *pka1 msl1* × **a** *msl1* (YSB1086 and YSB62), and α *cac1 msl1* × **a** *msl1* (YSB1084 and YSB62) (B); and WT α × WT **a** (H99 and KN99**a**), α *msl1* × **a** *msl1* (YSB13 and YSB62), α *cac2* × **a** *cac2* (YSB1065 and YSB1693), α *cac2* × WT **a** (YSB1065 and KN99**a**), α P_{H3}::*MSL1* × WT **a** (YSB1776 and KN99**a**), and α *cac2 msl1* × WT **a** (YSB1697 and KN99) (C). Mating cultures were photographed after 7 days (A and B) or 10 days (C) (magnification, ×100).

supplemental material), and the overexpression of *MSL1* was confirmed by Northern blot analysis (data not shown). Surprisingly, however, *MSL1* overexpression did not affect melanin production in the wild-type strain (see Fig. S4C in the supplemental material). Furthermore, the overexpression of *MSL1* did not increase the thermotolerance of wild-type *C. neoformans* but rather slightly decreased thermotolerance (see Fig. S4D in the supplemental material). *MSL1* overexpression did not particularly affect the heavy metal, antifungal drug, genotoxic, and oxidative stress resistances of the wild-type strain or the *cac1*Δ or *pka1*Δ mutants (data not shown). These data strongly imply that the artificial overexpression of *MSL1* does not affect normal cellular functions in *C. neoformans*. Since Msl1 contains just a series of WD40 repeats and does not appear to have any enzymatic, catalytic activity, the simple overexpression of *MSL1* may not trigger any phenotypic changes unless the expression level of its binding partner(s) is concomitantly increased.

Localization of Msl1 in *C. neoformans*. Based on the Yeast GFP Fusion Localization Database (http://yeastgfp.yeastgenome.org/index.php), Msi1 preferentially localizes to the nucleus in *S. cerevisiae*. When *MSI1* is overexpressed, however, Msi1 localizes to both the nucleus and cytoplasm (21), reflecting its multiple roles as a component of CAF-1 and as a signaling element regulating the Ras/cAMP pathway. To address the cellular localization of Msl1 in *C. neoformans*, we constructed an *MSL1*::*GFP-NEO* allele, in which GFP was fused in frame to the C terminus of Msl1, and integrated it into the native *MSL1* locus in the *msl1*Δ mutant. The Msl1-GFP fusion protein was functional because all *msl1*Δ mutant phenotypes were restored to WT phenotypes by the *MSL1*::*GFP* allele (data not shown). Similar to yeast Msi1-GFP, under normal, unstressed conditions, the Msl1-GFP fusion protein localized to both the nucleus and the cytoplasm but was more enriched in the nucleus (Fig. 7). Under stressed conditions, such as in the presence of an oxidative agent (diamide) or a high temperature (39°C), the cellular localization of Msl1-GFP was not significantly affected (Fig. 7). In summary, Msl1 is localized to both the nucleus and cytoplasm but is more enriched in the nucleus of *C. neoformans*.

Msl1 plays redundant and distinct roles with CAF-1 in *Cryptococcus*. The data accumulated thus far indicated that the Msl1-dependent signaling pathway appeared to play both cAMP-dependent and -independent roles largely independent of the Ras-signaling pathway in *C. neoformans*. Because Msi1/Cac3 is a component of CAF-1 in *S. cerevisiae* (24, 44), we addressed whether the pleiotropic roles of Msl1 are related to the functions of CAF-1. In budding yeast, CAF-1 consists of three factors: Rlf2/Cac1, Cac2, and Msi1/Cac3. Our BLAST search using the amino acid sequences of *S. cerevisiae* Rlf2/Cac1 and Cac2 revealed that *C. neoformans* contains an ortholog of Cac2 (CNAG_00718.2) with a score of 132.494 and an expectancy value of $1.41E^{-31}$, which is expected to encode an 813-amino-acid protein with multiple WD40 repeats, as observed for other Cac2-like proteins. In contrast, an ortholog of *S. cerevisiae* Rlf2/Cac1 was not apparent in the *Cryptococcus* genome database. Therefore, we decided to disrupt the *CAC2* gene in wild-type strains (H99 and KN99**a**) and

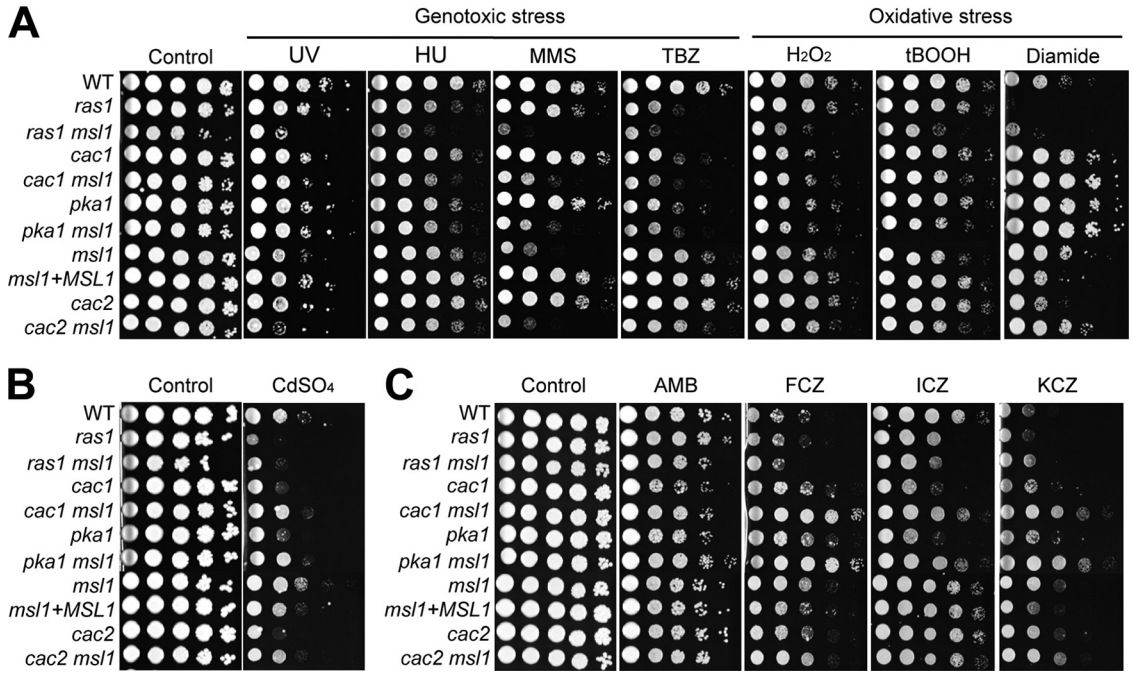

FIG 5 Msl1 is involved in diverse stress responses. Each *C. neoformans* strain (WT strain H99 and the *ras1*Δ [YSB53], *ras1*Δ *msl1*Δ [YSB1790], *cac1*Δ [YSB42], *cac1*Δ *msl1*Δ [YSB1084], *pka1*Δ [YSB188], *pka1*Δ *msl1*Δ [YSB1086], *msl1*Δ [YSB13], *msl1*Δ+*MSL1* [YSB528], *cac2*Δ [YSB1065], and *cac2*Δ *msl1*Δ [YSB1697] mutants) was grown overnight at 30°C in liquid YPD medium, 10-fold serially diluted (1 to 10^4 dilutions), and spotted (3 μl of the dilution) onto YPD agar containing 70 mM hydroxyurea (HU), 0.02% methyl methane sulfonate (MMS), 10 μg/ml thiabendazole (TBZ), 2 mM hydrogen peroxide (H_2O_2), 0.2 mM *tert*-butyl hydroperoxide (tBOOH) solution, or 4 mM diamide (A); 30 μM cadmium sulfate ($CdSO_4$) (B); or 0.8 μg/ml amphotericin B (AMB), 16 μg/ml fluconazole (FCZ), 0.05 μg/ml itraconazole (ICZ), or 0.2 μg/ml ketoconazole (KCZ). For UV sensitivity assays, the YPD plates containing cells were exposed to 300 J/m^2 of UV irradiation. Cells were incubated at 30°C for 72 h and photographed.

the *msl1*Δ mutants and compare their phenotypes with those of the *msl1*Δ mutant.

The deletion of the *CAC2* gene did not affect normal cell growth in either the WT or the *msl1*Δ mutant background (Fig. 2A). Unlike the *msl1*Δ mutant, however, the *cac2*Δ mutant did not show any growth defects at high temperatures or in response to membrane destabilization with SDS (Fig. 2), implying that the role of Msl1 in thermotolerance and cell membrane stability is largely independent of CAF-1 function.

CAF-1 mutants (*rlf2/cac1*Δ, *cac2*Δ, or *msi1/cac3*Δ) in yeast show genotoxic sensitivity because the CAF-1 complex functions in nucleotide excision repair and DNA damage protection (24). As described above, the *msl1*Δ mutant also exhibited increased sensitivity to UV and other DNA-damaging agents, such as HU and MMS (Fig. 5A), in *C. neoformans*. Interestingly, the deletion of *CAC2* did not significantly affect sensitivity to DNA-damaging agents such as HU, MMS, or TBZ (Fig. 5A). However, the *cac2*Δ mutant did show slightly elevated susceptibility to UV, and the *msl1*Δ *cac2*Δ double mutant exhibited even greater UV sensitivity than the *msl1*Δ or *cac2*Δ single mutant (Fig. 5A), indicating that Cac2 and Msl1 play redundant and additive roles in UV-mediated DNA damage repair.

We tested other Msl1-related phenotypes in the *cac2*Δ mutant. First, the levels of melanin biosynthesis and *LAC1* induction in the *cac2*Δ mutant appeared to be only slightly higher than those in the WT (Fig. 3C and D). The melanin levels in the *msl1*Δ *cac2*Δ mutant were almost equivalent to those in the *msl1*Δ mutant (Fig. 3D). These data indicate that Msl1 and Cac2 may play redundant roles in melanin production. The *cac2*Δ mutant was as efficient in capsule biosynthesis as the WT (Fig. 3E). Even the *msl1*Δ *cac2*Δ double mutant showed WT levels of capsule production (Fig. 3E). In sexual differentiation, WT levels of filamentous growth and mating were observed in bilateral matings between α *cac2*Δ and **a** *cac2*Δ mutants, showing that Cac2 is not required for mating, unlike Msl1 (Fig. 4D).

Similarly, the *cac2*Δ mutant did not exhibit any discernible phenotypes in diverse stress response and antifungal drug susceptibility assays (Fig. 5). The *cac2*Δ mutant displayed WT levels of susceptibility to most of the external stresses, except for $CdSO_4$ (Fig. 5B), which is in stark contrast to the *msl1*Δ mutant. In response to $CdSO_4$, the *cac2*Δ mutant showed increased sensitivity, which is opposite to the response of the *msl1*Δ mutant, which showed increased tolerance to $CdSO_4$ (Fig. 5B). The *msl1*Δ *cac2*Δ mutant was as resistant to $CdSO_4$ as the WT. In summary, Msl1 appears to play redundant roles with Cac2 only in the genotoxic stress response and melanin production but plays unique roles in mating, the stress response, and antifungal drug susceptibility, possibly without an involvement of CAF-1 function.

Msl1 is required for full virulence of *C. neoformans*. The involvement of Msl1 in virulence factor production and the diverse stress responses of *C. neoformans* prompted an investigation of its role in the virulence of *C. neoformans*. To address this question, a murine model of systemic cryptococcosis was utilized. The *msl1*Δ mutant was attenuated for virulence compared to the WT and complemented strains but eventually caused lethal infection (Fig. 8A). To address whether the attenuated virulence of the *msl1*Δ mutant is caused by reduced cell survival or the defective expression of virulence attributes in the host, we assayed the number of

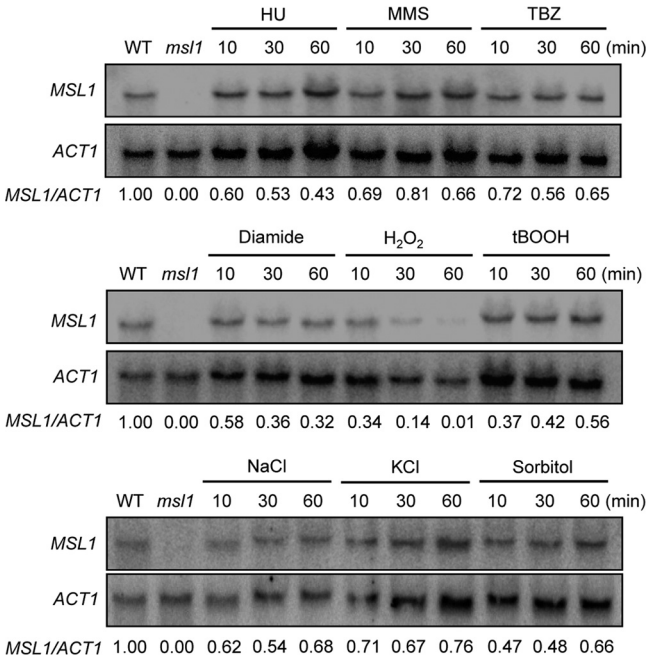

FIG 6 Expression patterns of *MSL1* in response to diverse external stresses. Northern blot analysis was performed with total RNA isolated from WT strain H99 grown in YPD medium containing genotoxic agents (70 mM HU, 0.02% MMS, or 7 μg/ml TBZ), oxidative damaging agents (2.5 mM diamide, 2.5 mM H_2O_2, or 0.3 mM tBOOH), and osmotic stress agents (1 M NaCl, 1 M KCl, or 1 M sorbitol). Total RNA isolated from the *msl1*Δ mutant served as a control. Each membrane was hybridized with the radioactively labeled *MSL1*-specific probe, washed, and developed with a phosphorimager. For the normalization of *MSL1* expression levels, the same membrane was stripped, rehybridized with the *ACT1*-specific probe, washed, and developed. The relative *MSL1* expression level (*MSL1/ACT1*) at each point indicates normalized *MSL1* expression levels compared to the level at the zero time point.

C. neoformans cells recovered from sacrificed animals. In all of the infected organs, including the lung, spleen, and brain, mice infected with the *msl1*Δ mutant appeared to show reduced cell counts compared to those of mice infected with the WT and its complemented strains, although these differences did not meet statistical significance (Fig. 8B). In particular, a reduction of cell numbers in the brain was more evident than in the lung and spleen. Taken together, Msl1 is required for the full virulence of *C. neoformans*.

Transcriptome analysis of Msl1-regulated genes. The finding that Msl1 plays pleiotropic roles in the growth, differentiation, stress response, and virulence of *C. neoformans* in a manner distinct from known signaling cascades prompted us to search for genes regulated by Msl1 on a genome scale. Therefore, we performed a transcriptome analysis of the *msl1*Δ mutant compared to the WT by using DNA microarray analysis. The expressions of a total 538 genes were found to be significantly differentially regulated ($P < 0.05$) between the WT and *msl1*Δ mutant strains (see Table S3 in the supplemental material). Among these, groups of genes involved in posttranslational modification, energy production and conversion, amino acid metabolism and transport, and signal transduction appeared to be overrepresented (Fig. 9A). Among these genes, only 17 (except *MSL1* itself) were upregulated (9 genes) or downregulated (8 genes) with changes of more than 2-fold in the *msl1*Δ mutant compared to the WT, indicating that Msl1 did not significantly affect basal transcript levels of genes in *C. neoformans*, unlike Ras/cAMP, in which 192 genes exhibited basal expression level changes of more than 2-fold (31). Among 47 genes whose expression was differentially regulated more than 1.5-fold, a majority of them (36 genes) have not been functionally characterized previously in *C. neoformans* (see Table S4 in the supplemental material), probably explaining the unique features of the Msl1-dependent pathway. Interestingly, genes whose functions have been studied in *S. cerevisiae* or *C. neoformans* include those involved in thermotolerance and stress responses, such as *HSP12* and *HSP122* (small heat shock proteins), *CAN2* (carbonic

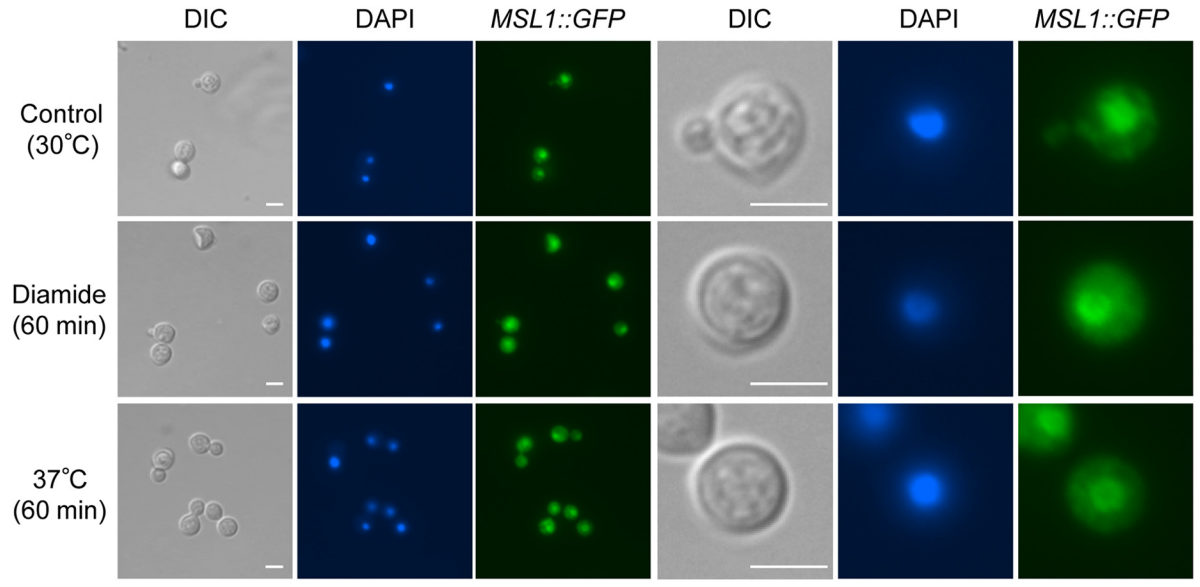

FIG 7 Cellular localization of the Msl1 protein in *C. neoformans*. The *C. neoformans MSL1*::*GFP* strain (YSB1918) was used to monitor the localization of Msl1, as described in Materials and Methods. Nontreated cells and cells grown at 37°C or treated with diamide were photographed. The white scale bars on the differential interference contrast (DIC) images indicate 10 μm.

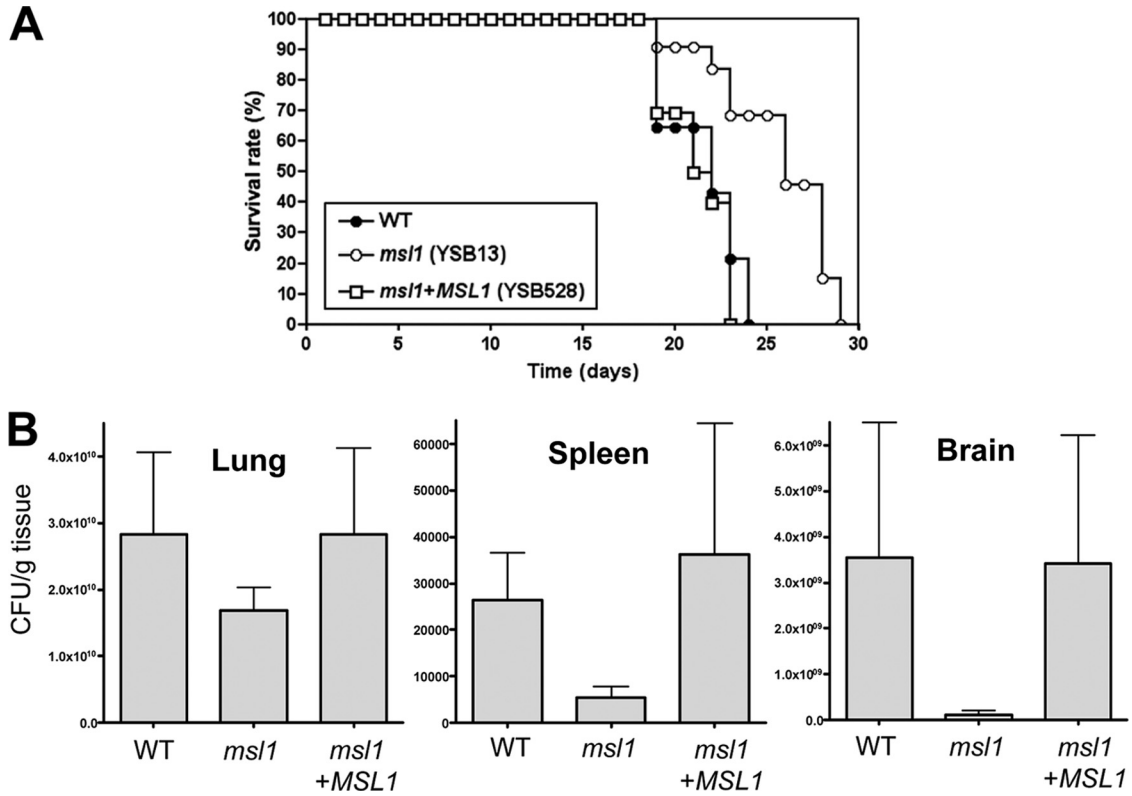

FIG 8 Msl1 is required for full virulence of *C. neoformans*. (A) A/J mice were infected with 5×10^4 cells of the α wild-type (H99), *msl1*Δ (YSB13), or *msl1*Δ+*MSL1* (YSB528) strain by intranasal inhalation. The *msl1*Δ mutant was less virulent than the other strains, and this difference was statistically significant ($P < 0.05$, calculated by the Mann-Whitney U test). (B) The CFU of surviving fungal cells in the spleens, lungs, and brains recovered from sacrificed animals (strain H99-infected mice sacrificed at days 19, 22, 23, and 24; *msl1*Δ mutant-infected mice sacrificed at days 19, 22, 23, 26, and 28; and *msl1*Δ+*MSL1* complemented strain-infected mice sacrificed at days 21, 22, and 23) were determined by serial dilution onto YPD medium. The error bars represent the standard deviations. Based on Bonferroni's multiple-comparison test, CFU differences among strains in all tissues were not statistically significant.

anhydrase), *PMP3* (a plasma membrane protein), *YVC1* (a vacuolar cation channel), *SNF3* (a glucose sensor), and *HSP78* (an oligomeric mitochondrial matrix chaperone), supporting the role of Msl1 in the regulation of stress responses in *C. neoformans* (Table 1). Among these genes, the upregulation of *HSP78* and the downregulation of *HSP12* by the deletion of *MSL1* were further confirmed by qRT-PCR and Northern blot analysis (Fig. 9B and C). Hsp12 is involved in AMB resistance, and its basal transcript levels are significantly reduced in both cAMP and HOG signaling mutants (26). Northern blot analysis revealed that basal expression levels of *HSP12* were also significantly reduced by the deletion of *MSL1* (Fig. 9C). In *S. cerevisiae*, Hsp78 encodes a mitochondrial heat shock protein belonging to the Clp family of ATP-dependent proteases (29). The expression of *HSP78* is highly induced by glucose starvation as well as heat shock (29). Although *SNF3* also appeared to be upregulated by the *msl1* mutation based on qRT-PCR data (Fig. 9B), its basal level of expression was barely detectable in either the WT or the *msl1*Δ mutants (data not shown). Interestingly, *HSP78* and *SNF3* are both glucose-repressed genes in yeast. Therefore, this observation appears to be correlated with the finding that the laccase gene (*LAC1*), which is induced by glucose starvation, was highly upregulated in the *msl1*Δ mutant (Fig. 3C). In conclusion, transcriptome profiles of the *msl1*Δ mutant exhibited only a limited overlap with those of the Ras/cAMP-signaling pathways, indicating that Msl1 may play a minor role, if any, in controlling the two signaling pathways. Nevertheless, the differential expressions of some stress-related genes, including molecular chaperone genes, support a role of Msl1 in the stress response and adaptation of *C. neoformans*.

DISCUSSION

This study identified and functionally characterized the *MSL1* gene, which encodes a yeast Msi1-like (MSIL) protein, with connections to the Ras/cAMP pathways and the putative chromatin assembly factor 1 (CAF-1) components in *C. neoformans*. To the best of our knowledge, the MSIL proteins have not been characterized in fungal pathogens previously. In fact, the closest yeast homolog of the *C. neoformans* Msl1 protein is Hat2, a subunit of the histone acetyltransferase complex, which is another yeast MSIL protein with WD40 repeats (16), rather than Msi1. Nevertheless, the WD40 domain arrangement of Msl1 is more homologous to that of yeast Msi1 than to that of Hat2 (Fig. 1B). Both Hat2 and Msi1 belong to the p48 protein family (also known as the retinoblastoma-binding protein RbAp48) (44). The p48 protein is one of three subunits of CAF-1 in humans and is more homologous to Hat2 than Msi1/Cac3. Nevertheless, only Msi1 copurifies with yeast CAF-1, indicating that Msi1 is one subunit of yeast CAF-1. With tblastn searches for either yeast Msi1 or Hat2 homologs in the *C. neoformans* genome database, Msl1 (CNAG_03297.2) was identified as the

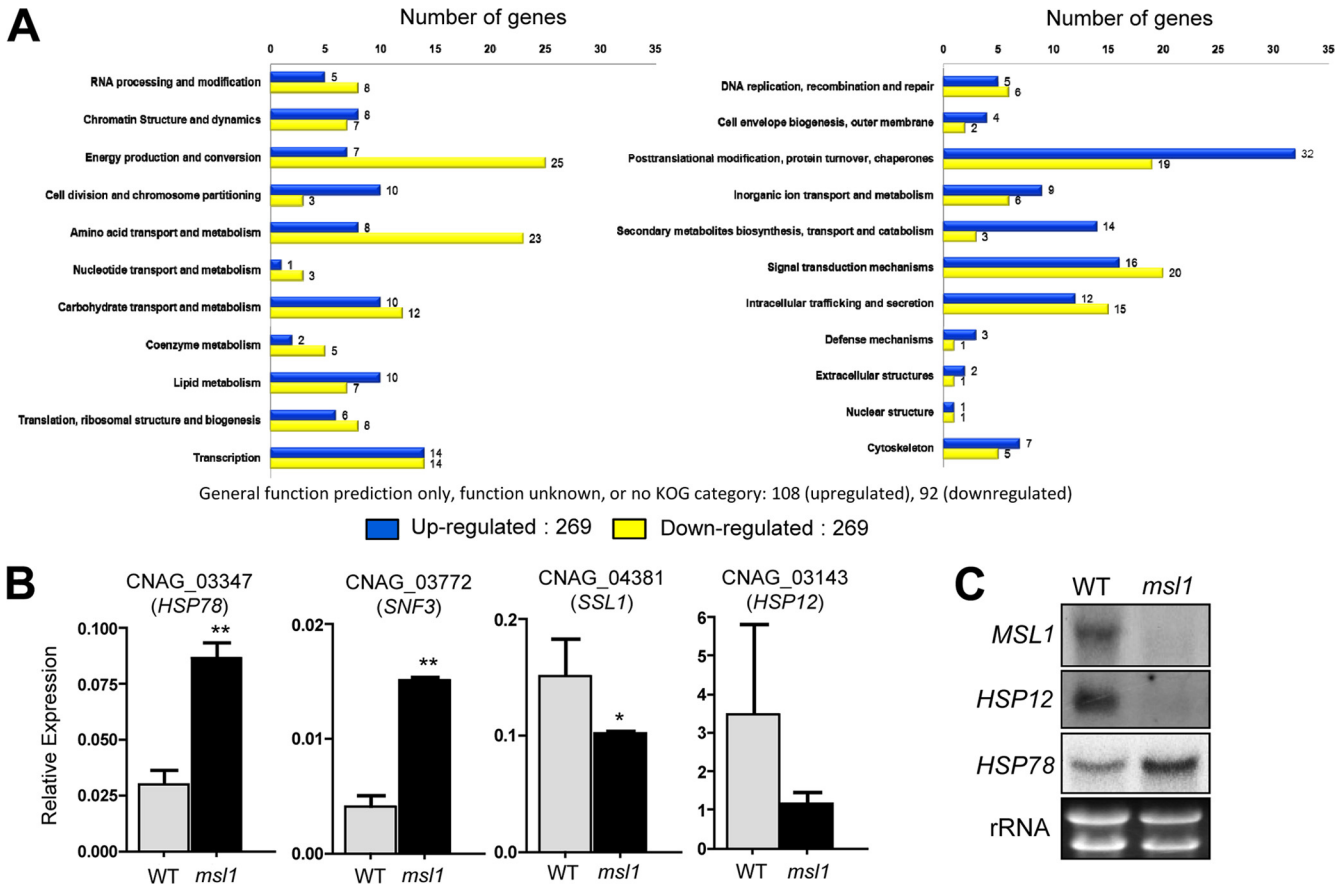

FIG 9 Identification of Msl1-dependent genes by transcriptome analysis. (A) Functional categorization of the genes regulated by Msl1. Genes whose basal expression levels in the *msl1*Δ mutant were significantly different from those in the WT ($P < 0.05$ by ANOVA) were functionally categorized based on KOG (eu*k*aryotic *o*rthologous *g*roups) functional descriptions (http://www.ncbi.nlm.nih.gov/COG). (B) For qRT-PCR, expression levels of each gene were normalized to those of *ACT1* as a control (the relative gene expression level is on the *y* axis). Statistical analysis was performed with the Student *t* test. A single asterisk indicates a *P* value of <0.05, and double asterisks indicate a *P* value of <0.01. (C) Northern blot analysis to verify expression patterns of *HSP12* and *HSP78*. For qRT-PCR and Northern blot analyses, the same total RNA set from WT strain H99 and the *msl1*Δ mutant (YSB13) prepared for the microarray analysis was used.

first and only significant hit, indicating that Msl1 is the only p48 protein family member found in *C. neoformans*. The genotoxic stress phenotype (UV sensitivity) observed for the yeast *msi1*Δ mutant, but not the *hat2*Δ mutant, is found in the *C. neoformans msl1*Δ mutant, suggesting that Msl1 appears to be the Msi1 ortholog. In future studies, however, it remains to be addressed whether Msl1 plays dual roles in both Msi1- and Hat2-like functions in *C. neoformans*.

Msl1 plays pleiotropic roles in the growth, differentiation, stress responses, and virulence of *C. neoformans* in both cAMP-dependent and -independent manners largely independent of Ras. Msl1 appears to negatively regulate the cAMP-signaling pathway, possibly upstream of the Cac1 adenylyl cyclase for melanin biosynthesis and mating. In contrast, Msl1 plays cAMP- and Ras-independent roles in sensing and counteracting diverse external stresses, such as high temperatures, cell membrane destabilizers, genotoxic and oxidative damaging agents, and toxic heavy metals. In *C. neoformans*, the Ras-signaling pathway is mainly independent of the cAMP-signaling pathway, except in the cases of invasive growth and mating (1, 31). This regulatory mechanism of Msl1 in *C. neoformans* is rather different from that of Msi1 in *S. cerevisiae*. Yeast Msi1 functions either between the Cyr1 adenylyl cyclase and PKA or downstream of PKA without directly affecting intracellular cAMP levels, PKA activity, or the expression of cAMP-dependent genes (21, 38, 46). It was suggested previously that yeast Msi1 sequesters and inactivates the Npr1 serine/threonine kinase to antagonize the ubiquitin-mediated degradation of several nutrient transporters, which subsequently activates the Ras/cAMP pathway (21). The Npr1 kinase has not been characterized in *C. neoformans*. Hence, it remains to be elucidated which signaling components in the cAMP-signaling pathway interact with Msl1 in *C. neoformans*.

The pleiotropic roles of Msl1 appeared to be partly related to the function of CAF-1 in *C. neoformans*. In *S. cerevisiae*, the mutation of any component of CAF-1 caused the following phenotypes: (i) increased sensitivity to UV or DNA-damaging agents and (ii) derepressed expression levels of genes in heterochromatic regions and the mating-type locus (14, 24). The disruption of any of the three *CAC* genes causes the same degree of UV sensitivity, and no additive effect was observed by the combinatorial mutation of the three genes. In *C. neoformans*, the deletion of *CAC2* (CANG_00718.2) not only slightly increased UV susceptibility compared to that of the WT but also further increased the UV sensitivity of the *msl1*Δ mutant, which differs from the case in *S.*

TABLE 1 List of Msl1-regulated gene having known functions

H99 locus tag	Fold change[a]	Gene (*S. cerevisiae* gene)[b]	Functional description
CNAG_04379	−2.843	(*VPS55*)	Late endosomal protein involved in late-endosome-to-vacuole trafficking
CNAG_03297	−2.344	*MSL1*	Msi1-like protein 1 in *C. neoformans*
CNAG_03143	−1.107	*HSP12*	Small heat shock protein orthologous to yeast Hsp12 in *C. neoformans*; regulated by the cAMP and HOG pathways and involved in antifungal drug resistance
CNAG_05144	−0.985	*CAN2*	Carbonic anhydrase; poorly transcribed under aerobic conditions and at an undetectable level under anaerobic conditions; involved in nonclassical protein export pathway
CNAG_01588	−0.789	(*PMP3*)	Small plasma membrane protein related to a family of plant polypeptides that are overexpressed under conditions of high-salt concn or low temp
CNAG_04879	−0.766	(*GDB1*)	Glycogen-debranching enzyme containing glucanotransferase and alpha-1,6-amyloglucosidase activities, required for glycogen degradation
CNAG_07368	−0.733	(*YVC1*)	Vacuolar cation channel; mediates release of Ca^{2+} from the vacuole in response to hyperosmotic shock
CNAG_01446	−0.727	*HSP122*	Small heat shock protein paralogous to *C. neoformans* Hsp12; regulated by the cAMP and HOG pathways and involved in antifungal drug resistance
CNAG_04381	−0.652	(*SSL1*)	Component of the core form of RNA polymerase transcription factor TFIIH
CNAG_07808	−0.594	(*AGX1*)	Alanine:glyoxylate aminotransferase; catalyzes the synthesis of glycine from glyoxylate, which is one of three pathways for glycine biosynthesis in yeast
CNAG_03772	0.892	(*SNF3*)	Plasma membrane glucose sensor that regulates glucose transport
CNAG_03347	0.922	(*HSP78*)	Oligomeric mitochondrial matrix chaperone that cooperates with Ssc1p in mitochondrial thermotolerance after heat shock; prevents the aggregation of misfolded matrix proteins

[a] Fold change indicates the $\log_2$(*msl1*Δ/WT) change. Genes having expression level changes of more than 1.5-fold are listed.
[b] Gene names in parentheses indicate *S. cerevisiae* gene names based on BLAST search results.

cerevisiae. These findings suggest that Msl1 and Cac2 either play redundant roles within the CAF-1 complex or independently contribute to DNA damage repair. Similarly, Cac2 is also partly involved in melanin production. In contrast, Cac2 appeared to be mostly dispensable for the role of Msl1 in mating, diverse stress responses, and antifungal drug susceptibility. In future studies, functional and structural relationships between Msl1 and Cac2 in *C. neoformans* should be further addressed. In yeast, Cac2 and Msi1/Cac3 do not interact directly with each other and are associated through binding to the largest component of the CAF-1 complex, Rlf2/Cac1. By lowering BLAST criteria, CNAG_01573.2 was found to be slightly homologous to yeast Rlf2/Cac1 (score = 38.9; E value = 0.003). Based on our preliminary data, interestingly, CNAG_01573.2 is one candidate Msl1-interacting protein (our unpublished data), suggesting that it is a potential candidate for the *Cryptococcus* Rlf2/Cac1-like protein. The functional and structural relationships among Rlf2, Cac2, and Msl1 in *C. neoformans* need to be further elucidated in future studies.

Regardless of the pleiotropic roles of Msl1 in the regulation of virulence factor and stress responses, the *msl1*Δ mutant exhibited only a minor defect in the virulence of *C. neoformans*. This may result from the complex nature of the *msl1*Δ mutant phenotypes. Increased high-temperature and genotoxic stress sensitivity could reduce the virulence of the *msl1*Δ mutant, whereas increased melanin production and enhanced resistance to certain oxidative stresses and a toxic heavy metal could contribute to enhance the survival of the *msl1*Δ mutant in the host. A similar example can be shown with HOG mutants of *C. neoformans*. The *hog1*Δ and *pbs2*Δ mutants are attenuated in virulence despite the fact that the mutants also exhibit an enhanced production of capsule and melanin (7). Although the reason for this is not fully understood, it is likely attributable to severe defects of the *hog1*Δ and *pbs2*Δ mutants in a variety of forms of stress response.

Our transcriptome analysis identifying Msl1-regulated genes further confirmed a role for Msl1 in stress responses and adaptation in *C. neoformans*. Several genes (*HSP78*, *SNF3*, *HSP12*, and *HSP122*) identified by a DNA microarray-based transcriptome analysis of the *msl1*Δ mutant serve as examples. However, it is notable that only a small subset of genes (17 genes having 2-fold changes and 47 genes having 1.5-fold changes) was identified despite the multiple roles of Msl1 in *C. neoformans*. This is in stark contrast to the Ras and cAMP mutants, in which 192 genes exhibited expression level changes of more than 2-fold based on our previous DNA microarray analyses (26, 31), further supporting that Msl1 plays a minor role, if any, in controlling Ras- and cAMP-signaling pathways in *C. neoformans*. The expression of *HSP12* and *HSP122* is known to be positively regulated by both the cAMP- and HOG-signaling pathways in *C. neoformans* (31). The disruption of both *HSP12* and *HSP122* affects antifungal drug resistance in the presence of salt shock. It remains elusive whether Msl1 controls the expression of *HSP12* and *HSP122* through the cAMP- and/or HOG-signaling pathways or other independent signaling pathways. Any functional or structural connection between those genes and Msi1-like proteins has not been noticed for other fungi as well as *Cryptococcus*. Therefore, a functional analysis of the target genes/proteins and their relationship with Msl1 remains to be explored.

In conclusion, our study provides a first report about the function of an MSIL protein in human fungal pathogens by using *C. neoformans* as a model system. Considering that a number of Msl1-related phenotypes in *C. neoformans* are unexpected based on studies of *S. cerevisiae* Msi1, the functions of MSIL-like proteins in other pathogenic fungi need to be investigated. Furthermore, the finding that the *C. neoformans* MSIL protein is involved in antifungal drug resistance as well as virulence suggests the possibility that fungal MSIL proteins may serve as novel antifungal therapeutic targets.

ACKNOWLEDGMENTS

We thank Andrew Alspaugh of Duke University for kindly providing *Cryptococcus* strains and plasmids. We also thank Jun-Tae Kwon for technical assistance.

This work was supported by National Research Foundation of Korea (NRF) grants funded by the South Korean government (MEST) (grant no. 2009-0058681, 2010-0029117, and 2008-0061963) to Y.-S.B. and NIH grants AI50438 to J.H. and AI080275 to K.N.

REFERENCES

1. **Alspaugh JA, Cavallo LM, Perfect JR, Heitman J.** 2000. *RAS1* regulates filamentation, mating and growth at high temperature of *Cryptococcus neoformans*. Mol. Microbiol. **36**:352–365.
2. **Alspaugh JA, Perfect JR, Heitman J.** 1997. *Cryptococcus neoformans* mating and virulence are regulated by the G-protein α subunit GPA1 and cAMP. Genes Dev. **11**:3206–3217.
3. **Alspaugh JA, Perfect JR, Heitman J.** 1998. Signal transduction pathways regulating differentiation and pathogenicity of *Cryptococcus neoformans*. Fungal Genet. Biol. **25**:1–14.
4. **Alspaugh JA, et al.** 2002. Adenylyl cyclase functions downstream of the Gα protein Gpa1 and controls mating and pathogenicity of *Cryptococcus neoformans*. Eukaryot. Cell **1**:75–84.
5. **Bahn YS, Cox GM, Perfect JR, Heitman J.** 2005. Carbonic anhydrase and CO_2 sensing during *Cryptococcus neoformans* growth, differentiation, and virulence. Curr. Biol. **15**:2013–2020.
6. **Bahn YS, Hicks JK, Giles SS, Cox GM, Heitman J.** 2004. Adenylyl cyclase-associated protein AcaI regulates virulence and differentiation of *Cryptococcus neoformans* via the cyclic AMP-protein kinase A cascade. Eukaryot. Cell **3**:1476–1491.
7. **Bahn YS, Kojima K, Cox GM, Heitman J.** 2005. Specialization of the HOG pathway and its impact on differentiation and virulence of *Cryptococcus neoformans*. Mol. Biol. Cell **16**:2285–2300.
8. **Bahn YS, et al.** 2007. Sensing the environment: lessons from fungi. Nat. Rev. Microbiol. **5**:57–69.
9. **Casadevall A, Rosas AL, Nosanchuk JD.** 2000. Melanin and virulence in *Cryptococcus neoformans*. Curr. Opin. Microbiol. **3**:354–358.
10. **Davidson RC, et al.** 2002. A PCR-based strategy to generate integrative targeting alleles with large regions of homology. Microbiology **148**:2607–2615.
11. **Dell EJ, et al.** 2002. The βγ subunit of heterotrimeric G proteins interacts with RACK1 and two other WD repeat proteins. J. Biol. Chem. **277**:49888–49895.
12. **D'Souza CA, et al.** 2001. Cyclic AMP-dependent protein kinase controls virulence of the fungal pathogen *Cryptococcus neoformans*. Mol. Cell. Biol. **21**:3179–3191.
13. **Enomoto S, McCune-Zierath PD, Gerami-Nejad M, Sanders MA, Berman J.** 1997. *RLF2*, a subunit of yeast chromatin assembly factor-I, is required for telomeric chromatin function *in vivo*. Genes Dev. **11**:358–370.
14. **Game JC, Kaufman PD.** 1999. Role of *Saccharomyces cerevisiae* chromatin assembly factor-I in repair of ultraviolet radiation damage *in vivo*. Genetics **151**:485–497.
15. **Granger DL, Perfect JR, Durack DT.** 1985. Virulence of *Cryptococcus neoformans*. Regulation of capsule synthesis by carbon dioxide. J. Clin. Invest. **76**:508–516.
16. **Hennig L, Bouveret R, Gruissem W.** 2005. MSI1-like proteins: an escort service for chromatin assembly and remodeling complexes. Trends Cell Biol. **15**:295–302.
17. **Hicks JK, Bahn YS, Heitman J.** 2005. Pde1 phosphodiesterase modulates cyclic AMP levels through a protein kinase A-mediated negative feedback loop in *Cryptococcus neoformans*. Eukaryot. Cell **4**:1971–1981.
18. **Hicks JK, D'Souza CA, Cox GM, Heitman J.** 2004. Cyclic AMP-dependent protein kinase catalytic subunits have divergent roles in virulence factor production in two varieties of the fungal pathogen *Cryptococcus neoformans*. Eukaryot. Cell **3**:14–26.
19. **Ishimaru N, et al.** 2006. Novel role for RbAp48 in tissue-specific, estrogen deficiency-dependent apoptosis in the exocrine glands. Mol. Cell. Biol. **26**:2924–2935.
20. **Jacobson ES.** 2000. Pathogenic roles for fungal melanins. Clin. Microbiol. Rev. **13**:708–717.
21. **Johnston SD, et al.** 2001. *CAC3* (*MSI1*) suppression of $RAS2^{G19V}$ is independent of chromatin assembly factor I and mediated by *NPR1*. Mol. Cell. Biol. **21**:1784–1794.
22. **Jullien PE, et al.** 2008. Retinoblastoma and its binding partner MSI1 control imprinting in *Arabidopsis*. PLoS Biol. **6**:e194. doi:10.1371/journal.pbio.0060194.
23. **Jung KW, Kim SY, Okagaki LH, Nielsen K, Bahn YS.** 2011. Ste50 adaptor protein governs sexual differentiation of *Cryptococcus neoformans* via the pheromone-response MAPK signaling pathway. Fungal Genet. Biol. **48**:154–165.
24. **Kaufman PD, Kobayashi R, Stillman B.** 1997. Ultraviolet radiation sensitivity and reduction of telomeric silencing in *Saccharomyces cerevisiae* cells lacking chromatin assembly factor-I. Genes Dev. **11**:345–357.
25. **Kennedy BK, et al.** 2001. Histone deacetylase-dependent transcriptional repression by pRB in yeast occurs independently of interaction through the LXCXE binding cleft. Proc. Natl. Acad. Sci. U. S. A. **98**:8720–8725.
26. **Ko YJ, et al.** 2009. Remodeling of global transcription patterns of *Cryptococcus neoformans* genes mediated by the stress-activated HOG signaling pathways. Eukaryot. Cell **8**:1197–1217.
27. **Kozubowski L, Lee SC, Heitman J.** 2009. Signalling pathways in the pathogenesis of *Cryptococcus*. Cell. Microbiol. **11**:370–380.
28. **Langfelder K, Streibel M, Jahn B, Haase G, Brakhage AA.** 2003. Biosynthesis of fungal melanins and their importance for human pathogenic fungi. Fungal Genet. Biol. **38**:143–158.
29. **Leonhardt SA, Fearson K, Danese PN, Mason TL.** 1993. *HSP78* encodes a yeast mitochondrial heat shock protein in the Clp family of ATP-dependent proteases. Mol. Cell. Biol. **13**:6304–6313.
30. **Lu X, Horvitz HR.** 1998. *lin-35* and *lin-53*, two genes that antagonize a *C. elegans* Ras pathway, encode proteins similar to Rb and its binding protein RbAp48. Cell **95**:981–991.
31. **Maeng S, et al.** 2010. Comparative transcriptome analysis reveals novel roles of the Ras and cyclic AMP signaling pathways in environmental stress response and antifungal drug sensitivity in *Cryptococcus neoformans*. Eukaryot. Cell **9**:360–378.
32. **McFadden DC, Casadevall A.** 2001. Capsule and melanin synthesis in Cryptococcus neoformans. Med. Mycol. **39**(Suppl 1):19–30.
33. **Nichols CB, Perfect ZH, Alspaugh JA.** 2007. A Ras1-Cdc24 signal transduction pathway mediates thermotolerance in the fungal pathogen *Cryptococcus neoformans*. Mol. Microbiol. **63**:1118–1130.
34. **Pratt ZL, Drehman BL, Miller ME, Johnston SD.** 2007. Mutual interdependence of *MSI1* (*CAC3*) and *YAK1* in *Saccharomyces cerevisiae*. J. Mol. Biol. **368**:30–43.
35. **Pukkila-Worley R, Alspaugh JA.** 2004. Cyclic AMP signaling in *Cryptococcus neoformans*. FEMS Yeast Res. **4**:361–367.
36. **Qian YW, Lee EY.** 1995. Dual retinoblastoma-binding proteins with properties related to a negative regulator of ras in yeast. J. Biol. Chem. **270**:25507–25513.
37. **Qian YW, et al.** 1993. A retinoblastoma-binding protein related to a negative regulator of Ras in yeast. Nature **364**:648–652.
38. **Ruggieri R, Tanaka K, Nakafuku M, Kaziro Y, Toh-e, Matsumoto AK.** 1989. *MSI1*, a negative regulator of the RAS-cAMP pathway in *Saccharomyces cerevisiae*. Proc. Natl. Acad. Sci. U. S. A. **86**:8778–8782.
39. **Smith TF, Gaitatzes C, Saxena K, Neer EJ.** 1999. The WD repeat: a common architecture for diverse functions. Trends Biochem. Sci. **24**:181–185.
40. **Solari F, Ahringer J.** 2000. NURD-complex genes antagonise Ras-induced vulval development in *Caenorhabditis elegans*. Curr. Biol. **10**:223–226.
41. **Spellman PT, et al.** 1998. Comprehensive identification of cell cycle-regulated genes of the yeast *Saccharomyces cerevisiae* by microarray hybridization. Mol. Biol. Cell **9**:3273–3297.
42. **Taylor-Harding B, Binne UK, Korenjak M, Brehm A, Dyson NJ.** 2004. p55, the *Drosophila* ortholog of RbAp46/RbAp48, is required for the repression of dE2F2/RBF-regulated genes. Mol. Cell. Biol. **24**:9124–9136.
43. **Vallim MA, Nichols CB, Fernandes L, Cramer KL, Alspaugh JA.** 2005. A Rac homolog functions downstream of Ras1 to control hyphal differentiation and high-temperature growth in the pathogenic fungus *Cryptococcus neoformans*. Eukaryot. Cell **4**:1066–1078.
44. **Verreault A, Kaufman PD, Kobayashi R, Stillman B.** 1996. Nucleosome assembly by a complex of CAF-1 and acetylated histones H3/H4. Cell **87**:95–104.
45. **Waugh MS, Vallim MA, Heitman J, Alspaugh JA.** 2003. Ras1 controls pheromone expression and response during mating in *Cryptococcus neoformans*. Fungal Genet. Biol. **38**:110–121.
46. **Zhu X, Demolis N, Jacquet M, Michaeli T.** 2000. *MSI1* suppresses hyperactive RAS via the cAMP-dependent protein kinase and independently of chromatin assembly factor-1. Curr. Genet. **38**:60–70.